Journal of Atmospheric and Solar-Terrestrial Physics 70 (2008) 2275–2292

Contents lists available at ScienceDirect

Journal of Atmospheric and Solar-Terrestrial Physics

journal homepage: www.elsevier.com/locate/jastp

Review

Fine structure of optical aurora

Ingrid Sandahl *, Tima Sergienko, Urban Brändström

Swedish Institute of Space Physics, P.O. Box 812, SE-981 28 Kiruna, Sweden

ARTICLE INFO

Article history:
Accepted 21 August 2008
Available online 26 September 2008

Keywords:
Optical aurora
Fine structure
Imagers
Filamentary aurora
Black aurora
Auroral ionosphere

ABSTRACT

This is a review paper on the fine structure of optical aurora. Spatial scales smaller than about 1 km and temporal scales shorter than about 1 s are considered. Fine structure is present in most types of aurora, but earlier much of it has not been possible to study properly due to instrument limitations. Recent advancements in optical instrumentation have provided considerable improvements of temporal and spatial resolution. Optical measurements are able to give higher resolution than any other types of ground-based instruments used in auroral studies. To interpret the information, both more advanced modelling and analysis methods are being developed. This gives access to new knowledge on the physical processes responsible for particle acceleration, precipitation, atmospheric ion chemistry, and auroral light production.

Contents

1. Introduction

Ever since the beginning of auroral research it has been known that aurora is extremely rich in fine structure. Spatial scales go down to tens of meters, corresponding to the electron gyro radius, and temporal scales down to fractions of a second (Maggs and Davis, 1968; Davis, 1978b; Borovsky et al., 1991). The character of the fine structure is different for different types of auroras.

We have considered here auroral forms with spatial scales smaller than about 1 km and temporal scales shorter than about 1 s. Small-scale structures are present

* Corresponding author. Tel.: +46 980 79084; fax: +46 980 79050.
E-mail address: ingrid.sandahl@irf.se (I. Sandahl).

1364-6826/$ - see front matter © 2008 Elsevier Ltd. All rights reserved.
doi:10.1016/j.jastp.2008.08.016

in most types of auroras caused by electrons. For example, there are narrow arcs and filamentary structures associated with discrete auroras. Black auroras, commonly appearing in a background of diffuse aurora, often have scales of hundreds of meters. The exact occurrence frequency of small-scale structures does not appear to have been measured. In proton auroras there may well be small-scale structures in the precipitating populations, but, because of charge exchange in the ionosphere, the resulting optical emissions will be spread out widely. Proton auroras have therefore not been included in this review.

The aurora is the footprint of events in the magnetosphere. It is often thought that the smallest auroral features do not map far out into the magnetosphere, but that they are caused by more local processes (Galperin, 2002). However, this does not mean that the auroral fine structure is unimportant for the large-scale behaviour of the magnetosphere. The fine structure of optical aurora is associated with fine structure in ionospheric properties, such as electron density and conductivity. Ionospheric feedback mechanisms contribute to magnetosphere—ionosphere coupling. For example, in a simulation by Streltsov and Lotko (2004) of the ionospheric Alfvén resonator the downward current region split up into several small-scale, intense current structures with alternating upward and downward currents. Such structures also appeared in a recent simulation by Streltsov (2007), where they seemed to be of the order of 1 km wide. A conclusion by Streltsov (2007) regarding the upward current region is that the ionosphere promotes narrowing and intensification of discrete auroral arcs and that this effect is strongest when the ionospheric conductivity is low. However, the parameters used in that simulation appeared to give an arc width of considerably more than 1 km. A complete review of work regarding ionospheric feedback studies is beyond the scope of this paper, but there is no doubt that the understanding of the ionospheric feedback and of its relative importance to magnetospheric physics is far from complete. In a review of results from coordinated studies using data from Cluster and ground-based instruments, Amm et al. (2005) pointed out that it has not yet been possible to resolve the important electron-scale plasma regime. They suggested that the electron scale may hold the key to understanding an increasing number of wave–wave and wave–particle mechanisms, and that these mechanisms may prove important for energy coupling and triggering of large-scale instabilities.

It is not clear how narrow auroral arcs are created. Borovsky (1993) reviewed 22 mechanisms for auroral arcs and concluded that none of them was able to explain widths of the order of 100 m. Many of the small-scale structures are thought to be related to nonlinear Alfvén wave phenomena (e.g. Lysak, 1990; Chmyrev et al., 1992). A review of dispersive Alfvén waves is given by Stasiewicz et al. (2000). Many Alfvén wave features were measured by Freja and FAST, but Stasiewicz et al. pointed out that simultaneous measurements of optical aurora and Alfvén waves were too rare to state with certainty how the two are connected. Chaston et al. (2003), using a data base of 1000 Alfvén wave events from FAST satellite data and calculating the resulting optical aurora, concluded that the most commonly occurring arc width caused by Alfvén waves is 900 m and that arcs of this width are also on average the most intense ones. Their calculations show that arcs less than 100 m can be due to Alfvén waves, but that such arcs will be quite weak. According to the measurements by Maggs and Davis (1968) the narrowest arcs are also the most intense ones and thus the results of Chaston et al. (2003) cast doubts about Alfvén waves as the mechanism for the narrowest structures.

For a long time limitations in instrument performance made it difficult to measure the finest spatial and temporal structures. Optical measurements were not able to keep up with the quickly changing shapes and colours. In the last couple of years the development of new detectors, in particular the electron multiplication charge coupled device (EMCCD), has opened up new possibilities to perform quantitative measurement with much better signal-to-noise ratio and faster readout time compared to conventional charge coupled devices (CCDs) (McWhirter, 2008). The higher sensitivity also allows measurements of weaker auroras and weaker emissions. An important point was made by Semeter et al. (2001b) who pointed out that "With respect to understanding the dynamic coupling between the magnetosphere and the auroral ionosphere the observational bias toward bright aurora is physically unjustified".

Optical measurements from satellites have been, and are, very important in the understanding of large- and medium-scale auroral phenomena, but for the smallest scales ground-based measurements are essential.

In Section 2 of this review we will describe instrumentation relevant for studies of auroral fine structure with emphasis on optical instruments. Some types of auroral fine structures are discussed in Section 3. In Section 4 conclusions and some ideas on the road ahead are given.

2. Instrumentation for studies of auroral fine structure

2.1. Ground-based imagers

A major problem in the study of small-scale optical aurora is to obtain instruments with sufficient temporal and spatial resolution and enough signal-to-noise ratio. Borovsky et al. (1991) analyzed the requirements for designing optical systems to measure aurora and list four such requirements: angular resolution, temporal resolution, light-gathering power, and data-recording convenience. The angular resolution needed is dictated by the smallest expected size of the structures to be measured. Borovsky et al. (1991) calculated the minimum possible arc thickness for a thin sheet of 5 keV electrons entering the atmosphere and obtained the result 9.5 m. Taking the sampling theorem into account and assuming that the arc profile is a Gaussian, this calls for a spatial resolution of 2.4 m to resolve the Gaussian properly. For a typical altitude of the lower edge of auroral arcs, 105 km, an angular resolution of 0.0016° is needed. The temporal

resolution requirement by Borovsky et al. (1991) was derived from typical velocities of auroral arcs, 100–200 m/s, and the time needed for an arc to move 9.5 m, 0.05 s. Fast variations have also been observed in flickering aurora. Typical frequencies are 3–20 Hz (Oguti, 1981; Sakanoi and Fukunishi, 2004), but there are also reports of much higher frequencies. The light-gathering power is a very critical point. When only a small part of the sky is imaged for a very short time not so much light is available. In addition, some of the most intense auroral emissions have a much longer lifetime than the desired temporal resolution. Therefore, it is often preferred to use prompt emissions, but this requires filters that will limit the amount of measurable light even more. The factors temporal resolution, spatial resolution, and light-gathering power are intimately tied to each other so that, for example, an increased spatial resolution may make it necessary to integrate measurements over a longer time period in order to obtain enough signal-to-noise ratio.

The all-sky cameras deployed in connection with the International Geophysical Year used black and white film and took one picture per minute. A typical exposure time was 1 s (Chamberlain, 1961). All-sky cameras were deployed at more than 100 sites (Akasofu, 2007), and they led to very important results regarding the global auroras, most notably the auroral oval (Korosheva, 1962; Feldstein, 1963) and the auroral substorm (Akasofu, 1968). But the temporal resolution, in particular, made them useless for studies of auroral fine structure. Actually, for a long time the human eye was the best instrument to observe fast temporal developments of auroral forms.

With the advent of TV cameras with image intensifiers the situation was drastically improved. In Alaska Davis and Hicks (1964) used an Image orthicon tube and in Canada Scourfield and Parsons (1969) used a Vidicon system. These cameras operated at video frame rates, 25–30 frames per second, but with rather poor dynamic range and signal-to-noise ratio. The field of view depended on the lens used. The system of Davis and Hicks (1964) had a field of view of 16° and the system of Scourfield and Parsons (1969) had normally 33°. Now the temporal and spatial behaviour of the small-scale structures could be established, at least for the part of the image close to magnetic zenith. To obtain absolute intensities it was common to combine the TV images with measurements from photometers. Improved types of intensified TV cameras were developed and in particular the intensifier silicon-intensified target (ISIT) tube found wide use in auroral studies from the mid-1980s.

In more modern auroral TV cameras intensified charge coupled device (ICCD) detectors are used. Examples of such systems are the mobile, campaign-oriented instruments Portable Auroral Imager (PAI) of the University of Calgary (Trondsen and Cogger, 1997) and the Odin (Optical Digital Imager) of the University of Tromsø (Blixt et al., 2005b). With a 50 mm lens the maximum resolution at 105 km altitude is better than 40 m. When emissions are weak, integration may be needed. For low light phenomena the resolution of PAI at auroral altitudes is in practice about 100 m. PAI gives 30 frames per second and uses an exposure time of 1/60 s, that is 0.017 s. Odin gives 25 frames per second.

An auroral-arc-imaging system designed by Borovsky et al. (1991) had a resolution of 2.1 m for bright and 10.5 m for dim objects at 105 km altitude. This system consisted of an intensified charge injection device (CID) television camera attached to a 10-inch f/6.3 Schmidt–Cassegrain telescope. CID is a solid-state detector quite similar to a CCD detector. The frame rate was 30 per second and the image forming time 1/60 s.

The colours of the aurora contain much information. For example, emission intensity ratios depend on the primary particle distribution. In ground-based studies of aurora so far the three strongest emissions dominate. These are the red O(^{1}D) and green O(^{1}S) emissions at 630.0 and 557.7 nm and the blue N_2^+ 1NG system at 427.8 nm. They are fairly easy to use, since they are usually intense and not contaminated by other emissions. However, other emissions have great potential to give important information, and with improved optical instruments more emissions are now being explored (Semeter, 2003).

For a long time colour film was used in all-sky cameras. Colour images give some information about what the aurora looked like, that is not available from filtered images. A few all-sky or near all-sky imagers now use colour CCDs. Such imagers can be relatively inexpensive. The observatory imager at the Swedish Institute of Space Physics is a standard Fuji digital camera (Brändström, 2003). For most images the exposure time is 6 s. RAINBOW (Syrjäsuo et al., 2005) is an imager developed at the University of Calgary, which is based on a Starlight Xpress camera originally intended for astronomy. In the fast readout mode it can give one image every 3 s with a resolution of 752 × 290 pixels. It records the images using four wide-band channels, cyan–magenta, cyan–green, yellow–magenta, and yellow–green, and the images can be used for approximate reconstructions of the 557.7, 630.0, and 427.8 nm emissions (Partamies et al., 2007).

A problem with the two oxygen emissions, above all the red line, is the long lifetime. This is obvious for the red line with its lifetime of 120 s, but also the green line lifetime, 0.7 s, is much longer than the time for each TV frame and will obscure fast temporal variations. Therefore, TV cameras are sometimes equipped with filters blocking all wavelengths below about 650 nm (Frey et al., 1996b; Trondsen et al., 1997; Lanchester et al., 1998; Blixt et al., 2005a). This makes it possible to obtain sharp images of prompt infrared emissions in the N_2^+ Meinel and $N_2$1PG bands.

For measurements at a specific wavelength, usually narrow-band interference filters are used. Often several wavelengths are of interest and it is common to use a filter wheel. Interference filters only work as specified for a rather limited range of incidence angles, and therefore it is common to use a telecentric lens system that makes all cone beams as perpendicular as possible to the filter surface. This is especially important for systems with a wide opening angle (Mende et al., 1977). For systems with a sufficiently small field of view the narrow-band filter can be mounted in front of the lens. For a bandwidth of 2 nm this works for a field of view of ±7.5° or less. This is applied in HAARPOON (HAARP Optical Observing

Network) near the HAARP (High Frequency Active Auroral Research Program) facility in Alaska (Pedersen et al., 2008). By combining a camera with 15° field of view with a large curved mirror of the type used at road intersections, a total field of view of 60–90° is achieved. This design is considerably less expensive than a conventional telecentric lens system.

Some systems allow simultaneous imaging through different filters onto the same detector. The Simultaneous Multispectral Imager (SMI) (Semeter et al., 2001a) measures at four different wavelengths with 22° diagonal field of view, giving a spatial resolution of 300 m at 100 km altitude. The all-sky imagers of the Automatic Geophysical Observatory (AGO) network in Antarctica have dual optics imaging the 427.8 and 630.0 nm emissions simultaneously onto the same CCD (Mende et al., 1999).

The high temporal resolution of ICCD detectors comes at a cost. The photocathode of the image intensifier has considerably lower quantum efficiency as compared to the bare CCD (CCD without image intensifier), and that lower quantum efficiency will determine the quantum efficiency of the whole system. Also, the linearity of the ICCD detector will be impaired so that the accuracy in absolute intensity measurements will be much lower. Furthermore, the ICCD has a much lower dynamic range as compared to a CCD.

An example of a system without image intensifiers is the Auroral Large Imaging System (ALIS) in northern Scandinavia (Steen, 1989; Brändström, 2003). ALIS was designed to measure the three-dimensional luminosity distribution and consists of six stations with overlapping fields of view so that tomography-like inversion can be used (Gustavsson, 1998, 2000). ALIS imaging detectors are thinned backside illuminated CCDs with six-position filter wheels and interference filters. The imagers can be pointed to any direction and the whole system is remote controlled via internet. The maximum spatial resolution at 100 km is 100 m, typical exposure time 1–2 s, and typical temporal resolution 5 s. This system allows measurements of absolute intensities with accuracy comparable to that of photometers. HAARPOON (Pedersen et al., 2008) in Alaska also uses bare CCDs. HAARPOON has three stations with two imagers (Apogee Alta E47) with fixed filters at 557.7 and 630.0 nm at each station. Images of 256×256 pixels are obtained. The camera is placed 2 m away from the mirror and views it obliquely so that no part of the sky image is obscured by the camera. Geometrical correction is then carried out using the star background.

During the past few years electron multiplication CCDs (EMCCDs) have become an increasingly interesting alternative to both image-intensified CCDs and bare CCDs (McWhirter, 2008). These devices provide an on-chip gain that practically eliminates the readout noise, thus enabling very high frame rates with good signal-to-noise ratio. Recently, thinned backside-illuminated EMCCD imagers with relatively large pixels have become available.

Auroral Structure and Kinetics (ASK) is a powerful instrument for high-resolution measurements (Ashrafi, 2007; Dahlgren et al., 2008). It consists of three separate Andor iXon EMCCD cameras with lens systems giving a field of view of $6.1 \times 6.1°$, corresponding to 10×10 km at 100 km altitude. The spatial resolution at this height is 20 m and the temporal resolution several frames per second. The three cameras have interference filters giving three narrow passbands. ASK 1 is mainly aimed at E-region aurora and measures O_2^+ first negative band at 562.0 nm. ASK 2 measures the F region O^+ emission at 731.9 nm, to some extent contaminated by OH airglow and the N_2^+ 1 PG bands. ASK 3 measures the O emission at 777.4 nm that originates from both the E and the F region. Absolute intensity calibration is carried out using reference stars.

Imagers designed to measure small-scale structures see only a small part of the sky. To obtain the larger context of the auroral morphology and evolution they need to be accompanied by imagers with a much larger field of view. Present day all-sky camera systems are for example the THEMIS all-sky imaging array (ASI) (Donovan et al., 2006) in North America, MIRACLE (Syrjäsuo, 2001) in Northern Scandinavia and Svalbard, and ITACA^2 (Massetti, 2005) with one camera on Svalbard and one on the east Greenland coast. The THEMIS imagers have non-intensified panchromatic CCDs and no filters. THEMIS ASI is the largest imager array in operation and covers the whole auroral zone over the North American continent. It was planned as an important complement to the NASA THEMIS (Time History of Events and Macroscale Interactions during Substorms) satellite mission. MIRACLE imagers have intensified CCDs and seven position filter wheels. The field of view of an all-sky imager corresponds to 600 km at an altitude of 110 km. Typical spatial resolution in zenith is 1 km or a little more at 110 km altitude and typical exposure time 1 s. The same type of imager is used in ITACA^2. MIRACLE is now being upgraded with EMCCD imagers at two stations and non-intensified CCD imagers at two stations.

There are several imagers and imaging systems in addition to those mentioned here. An overview including web links of optical instruments and instrument networks for auroral measurements is found at www.irf.se/auropt.

2.2. Meridian scanning photometers and spectrographs

A majority of the imagers do not perform absolute intensity measurements. Optical instruments measure the so-called apparent emission rate. This is usually expressed in rayleighs (R) (Hunten et al., 1956; Chamberlain, 1961; Baker and Romick, 1976) where one R is the apparent emission rate of 10^{10} photons/(s m^2 column). Apparent emission rates are given for single lines or specified wavelength intervals. Thus absolute calibration is mainly carried out for imagers operating with narrowband filters. Absolute calibration of imagers has been described by, for example, Kosch et al. (1998), Kaila and Holma (2000), Yamamoto et al. (2002), and Taguchi et al. (2004).

If there are different emissions in the wavelength region within a filter passband, additional information is needed to determine their relative contributions. For white light measurements this is even more important.

Imagers working in white light measure everything within a very large wavelength interval, and are not suitable, nor even intended, for absolute measurements. Thus imagers are often operated together with photometers, meridian scanning photometers, and/or spectrographs. For studies of medium-scale features meridian scanning photometers have also frequently been the main optical instruments, but for small-scale structures the temporal and spatial resolution is insufficient for such use. For example, the meridian scanning photometer at Ny Ålesund, Svalbard, has a 2° field of view and a meridian scan over 160° takes 18 s (Moen et al., 1993).

When using photometer data it is important to take the size of the photometer field of view into account, since small-scale auroras may only cover a part of it. For example, in a study by Lanchester et al. (1998) the field of view of a photometer was 0.5°, corresponding to almost 1 km at auroral altitudes, while the investigated small-scale structures had a width of about 100 m.

Auroral spectrographs achieved a high spectral resolution very early. Already in the 19th century the resolution was about 1 nm. To be able to record weak emissions also very long exposure times were used. In auroral studies in Spitsbergen 1899–1900 by Jonas Westman and Josef Sykora exposure times from 1 to as much as 28 h were used (Chernouss and Sandahl, 2008).

The High Throughput Imaging Echelle Spectrograph, HiTIES, (Chakrabarti et al., 2001) was designed for high sensitivity and has been used in several studies of small-scale aurora. HiTIES has a slit of 8°, at least 0.1 nm spectral resolution, and a typical integration time of 30 s. The spectral resolution is sufficient to measure Doppler shifts of emitting particles. HiTIES can simultaneously image 5–20 spectral intervals that the user can select anywhere in the spectrum between 400 and 1000 nm. The ability to obtain spectra from separated intervals simultaneously was innovative. HiTIES has been used at Søndre Strømfjord and in the Spectral Imaging Facility (SIF) on Svalbard (Lanchester et al., 2003).

In spectrographs the wavelengths are usually separated by gratings. A different approach was applied in a spectrometer developed by Shiokawa et al. (2002), who used an acousto-optic tunable filter, AOTF. This filter consists of a TeO_2 crystal to which an RF frequency is applied. Frequencies from 180 to 100 MHz give passbands between 450 and 700 nm with a bandwidth of 2–3 nm. The tuning is controlled by a personal computer. A full scan of a 10 kR aurora can be done in 100 s, but it is also possible to select just a few desired wavelength intervals and perform a much faster scan.

2.3. Incoherent scatter radars

In many studies of small-scale structures results from incoherent scatter radars are essential. The EISCAT mainland UHF radar system (www.eiscat.org) is the only instrument that can measure ion drift at high temporal and spatial resolution and thus give detailed information about the horizontal electric field. The temporal resolution depends on the measurement program. So far a resolution of 0.2 s has been achieved in tristatic measurements with the UHF radar. The UHF radar beam has a half width of 0.6°, corresponding to less than 1 km at 100 km altitude. With AMISR (advanced modular incoherent scatter radar) naturally enhanced ion acoustic lines (NEIALs) were measured with a time resolution of 19 ms (Michell et al., 2008). The AMISR radar beam width is $1 \times 1°$, that is 1.7×1.7 km at 100 km altitude.

2.4. Instruments on satellites

Our present day understanding of auroral physics is largely due to research using satellite instruments, but for small-scale structures satellite measurements are not nearly as useful as they are for medium- and large-scale phenomena. There are two reasons for this (e.g. Borovsky et al., 1991). Firstly, since satellites are moving while they are measuring it is not possible to distinguish between temporal and spatial variations from single satellite measurements. Secondly, the high velocity, about 7 km/s, combined with realistic data rates lead to insufficient resolution for studies of the smallest structures. Still, satellite measurements can be valuable in studies of small-scale structures. Ground-based instruments can give the temporal and spatial history of an event, but they cannot make direct measurements of the primary particle distribution, parallel currents, or potential drops above auroral structures. In-situ measurements by a satellite passing above an auroral structure is likely to give information about the quality of assumptions made in the data analysis and set limits for the choice of possible mechanisms. In this section we will summarize the capabilities of different satellite instruments in relation to small-scale aurora studies.

No satellite imager has so far been able to give a resolution good enough to resolve small-scale structures. The first satellite imager to obtain 2D images in which all pixels were exposed at nearly the same time was the UV Imager on Viking (Anger et al., 1987). Its temporal resolution was 20 s, one image per satellite spin, and the exposure time 1 s. With Viking the development of the global aurora could be followed with higher temporal resolution than ever before. The imagers on Freja (Murphree et al., 1994) had much better spatial and temporal resolution than Viking, but, due to the much lower altitude of the orbit, Freja did not give the global overview. Freja had apogee at 1800 km and Viking at 14,000 km. The Freja detectors were intensified CCD detectors with 228×385 pixels. The field of view was $22.4 \times 30°$ and the spatial resolution at apogee about 5 km. One picture was obtained in each satellite spin, that is every 6 s, and the exposure time was 0.37 s. One camera obtained images in the LBH band, 134–180 nm, and the other in the range 130.4–1250 nm.

Freja also carried out high-resolution particle and field measurements. For particles the resolution corresponded to hundreds of meters at auroral altitudes and for electric and magnetic fields the resolution was in the 1–10 m range (Lundin et al., 1998).

The DMSP Operational Linescan System images (http://www.ngdc.noaa.gov/dmsp/sensors/ols.html) have a spatial resolution of about half that of Freja, but these

satellites only obtain one image per 6 h orbit. The Global Ultraviolet Imager (GUVI) in the NASA TIMED mission is an imaging spectrograph that obtains one image per pass in each of up to five selectable wavelength bands in the range 120–180 nm with a resolution of 7×7 km at nadir at an altitude of 150 km (Christensen et al., 2003).

The imagers on Polar (Frank et al., 1995; Torr et al., 1995) and IMAGE (Mende et al., 2000a–c; Sandel et al., 2000) were designed to obtain global overviews of the aurora and could not resolve small-scale structures. As an example, the Wideband Imaging Camera on IMAGE had a resolution at apogee of about 50 km.

The FAST satellite was specifically designed to investigate the microphysics of the aurora (Pfaff et al., 2001). It has a highly elliptical orbit with apogee at 4175 km and perigee at 350 km. For particles the best resolution corresponds to a few hundred meters at auroral altitudes. Probe measurements can give the electron density with a resolution better than 10 m and the three axis magnetic field is obtained with a resolution corresponding to about 10 m. There is no imager and FAST is a single spacecraft, so there is normally a problem of distinguishing between temporal and spatial variations and to put the measurements into a context for small-scale structures.

The Japanese microsatellite Reimei, previously (before launch) named INDEX, carries a payload especially designed to investigate the fine structure of aurora (Saito et al., 2001). Reimei was launched in August 2005 and flies in a circular near polar orbit at an altitude of 630 km. There are two scientific instruments, the multichannel auroral camera, MAC, (Sakanoi et al., 2003) and the electron and ion spectrum analyzer, EISA (Asamura et al., 2003). MAC has three channels equipped with interference filters at 428.2, 558.0, and 671.7 nm to measure the N_2^+ first negative band, O(^{1}S) 557.7 nm, and the N_2 first positive band. The CCD chips have 1024×1024 pixels, but to obtain high sensitivity normally binning of 8×8 is used. The camera is either pointed down the field line to measure the aurora at the foot point of the particle instrument (mode S) or pointed towards the limb (mode H). In mode S the spatial resolution is 1.2×1.2 km at 100 km giving an 80×80 km picture. One picture is taken by each camera every 120 ms with 40 ms exposure time. The particle instrument EISA measures electrons in the energy range 12 eV–12 keV and ions from 10 eV/q to 13 keV/q. The temporal resolution is 20 ms for 16 energy steps and 40 ms for 32 energy steps. The time interval 20 ms corresponds to 150 m.

Ground-based measurements and measurements on satellites complement each other, and in the ideal situation they are on the same magnetic field line. Unfortunately, due to the small field of view of high-resolution ground-based optical instruments, good conjunctions are rare. As an example, during the month of February 1997 there was only one conjunction between FAST and the ground station at Poker Flat. A way to get around this is to fly cameras on aircraft, as was done by Stenbaek-Nielsen et al. (1998) and Peticolas et al. (2002). They performed measurements conjugate to FAST from a Sabre-60 jet aircraft with an all-sky camera and narrow angle cameras. Results from three events are discussed in their papers. An additional advantage of using aircraft is the possibility to get above the clouds. An all-sky image of an arc system studied during one of the events together with particle data is shown in Fig. 1, taken from Stenbaek-Nielsen et al. (1998).

3. Topics in auroral fine structure

In this section we will discuss fine structure in some selected types of auroras: narrow auroral arcs, auroral curls and filaments, auroral rays, and black aurora. These are not the only auroral types displaying fine structure, but these are the ones that have so far received most attention.

3.1. Narrow auroral arcs

To evaluate different mechanisms for auroral arc formation, correct information about the distribution of arc widths is necessary. Measurements of the width of optical auroral arcs have been carried out for a long time, but this task is more complicated than it seems at first sight and it has not yet been solved sufficiently. Accurate measurements can only be done along the magnetic field line, apparent widening is caused by arc motion combined with long lifetimes of strong emissions, and very narrow features may exist for just a short time so that the sensitivity of the imager is insufficient.

According to the work of Maggs and Davis (1968) the most probable width of an elemental arc is less than 100 m, which is equal to the electron skin depth at 1000–2000 km altitude. Later inspection of the data of Maggs and Davis suggests that many of their measurements were obtained in diffuse aurora (Stenbaek-Nielsen et al., 1999). Borovsky et al. (1991) observed arc thicknesses of as little as 40 m, although typical values were found to be 100 m.

Knudsen et al. (2001) used all-sky camera data to study the widths of 3126 stable arcs measured at 557.7 nm. The spatial resolution of the measurements was 1.7 km at 135 km altitude but the narrowest arcs found were 8 km wide. At the measured resolution no significant fine scale was found inside the meso-scale arcs. These observations led Knudsen et al. to suggest that there is a gap in arc widths between the arcs measured by them and the arcs measured by Maggs and Davis (1968), and that the processes responsible for forming fine-scale arcs are different from the processes responsible for wider arcs.

In order to resolve the question of a possible gap in arc widths, a camera system named DAISY, Dense Array Imaging SYstem, was designed at the university of Calgary (Partamies et al., 2008) This system consists of three colour CCD cameras, one with a 20° field of view looking up along the magnetic field line, and two with 90° field of view viewing the aurora from the side. The narrow angle camera has a resolution of 100 m at 135 km altitude and tomography-like inversion will be used to analyze the data. A campaign in 2006 with a prototype camera with 400 m spatial resolution resulted in observations of 31 arcs with widths in the range of 1.9–14 km. A campaign

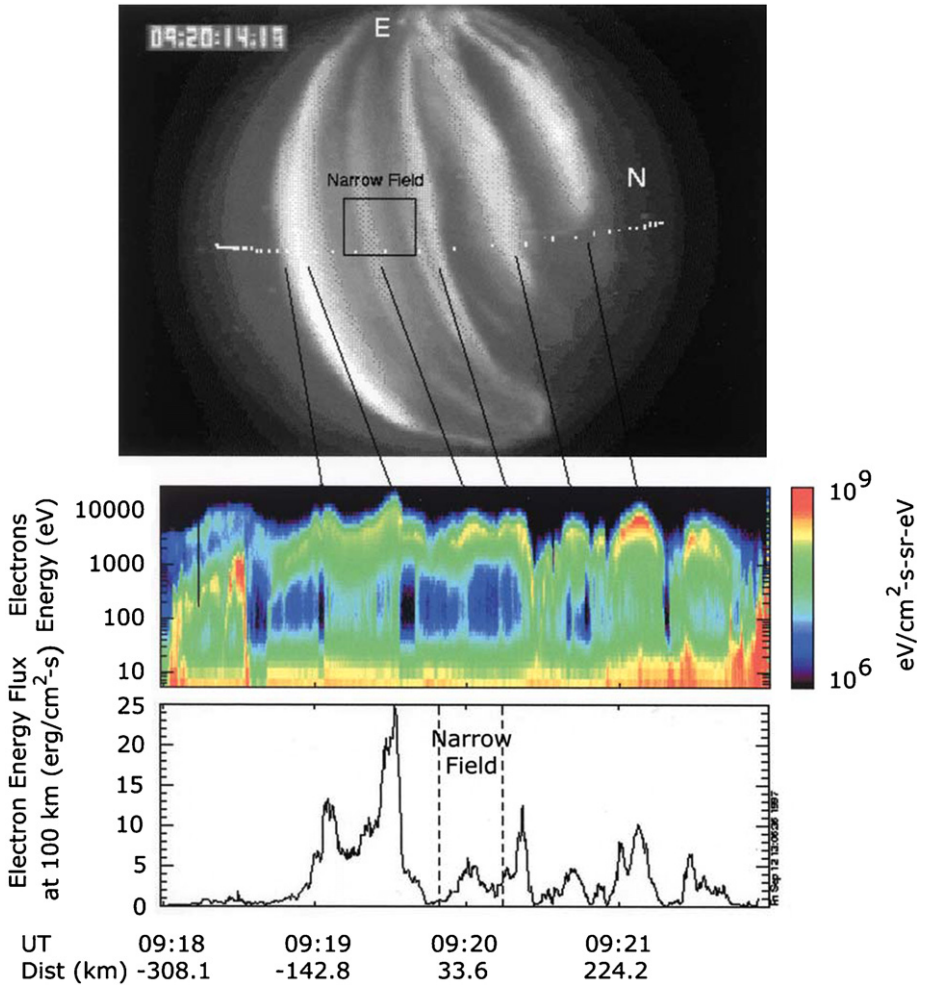

Fig. 1. Conjugate measurements of optical aurora and auroral electrons. In order to obtain good conjugacy with FAST imagers were flown on an aircraft. This all-sky image gives an overview of the situation. The dotted line shows the projected satellite orbit and the small square the field of view of one of the narrow-angle imagers. There was very good correspondence between the electron energy flux measured by FAST and the auroral arcs (from Stenbaek-Nielsen et al., 1998). Reproduced by permission of American Geophysical Union.

with the complete DAISY was carried out in 2007. Analysis of data from the 20° camera gave 500 thin arc structures. Of these, 70 per cent were in the size range of the suggested gap in arc widths, 0.5–1.5 km (Partamies, personal communication 2008). Fig. 2 shows the distribution of widths obtained by the different studies. Even though the size ranges overlap, it is probably impossible to determine the actual size distribution from these measurements.

When comparing data on arc widths it is important to pay attention to the temporal resolution of the measurements. Narrow arcs tend to have shorter lifetimes. The arcs studied by Knudsen et al. (2001) had an average lifetime of 3 min, while Partamies et al. (2008) obtained an average lifetime of 1 min.

In space, a wide range of scales is found in current structures, and studies using in situ data show no indication of a gap in the size distribution. In data from Freja with apogee at 1700 km the width of field-aligned current structures went from 500 km down to less than

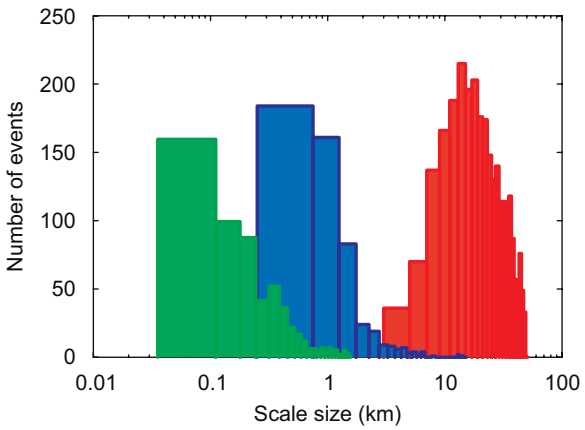

Fig. 2. Widths of auroral arcs. Distributions of widths of auroral arcs found in the studies by Maggs and Davis (1968) (peak to the left), Knudsen et al. (2001) (peak to the right) and with the new DAISY system (peak in the middle) (Noora Partamies, personal communication).

100 m with the highest current densities for the smallest-scale size currents (Stasiewicz and Potemra, 1998). The suggested cause for the small-scale currents was inertial Alfvén waves excited at heights less than 1 R_E above Freja. Observations of Alfvén waves by FAST confirm the observations by Freja (Stasiewicz et al., 2000). According to FAST the Alfvén waves are most common in and around the cusp, but they are not unusual in the nightside. They are not seen where electrostatic potentials exist below FAST (perigee at 350 km and apogee at 4180 km) and rarely in regions of inverted V electrons.

The electric field of shear Alfvén waves has a component parallel to the magnetic field, and this component is able to accelerate electrons. Shear Alfvén waves have been used quite successfully to explain multiple fine-scale structures. Dispersion of shear Alfvén waves can cause an arc to cascade. This was observed by Semeter and Blixt (2006). They used an intensified white light TV camera and applied a special analysis method so that the frame rate could be doubled to 50 frames per second. One initial arc cascaded into multiple arcs in less than 0.5 s, as shown in Fig. 3.

In fact, multiple arc systems are common features. Hallinan and Davis (1970) and Davis (1978b) described symmetric multiple systems with a central stationary arc, westward drifting arcs equatorward of the central arc, and eastward drifting arcs poleward of the central arc. Trondsen et al. (1997) found that asymmetric arrays of multiple parallel arcs are common during disturbed conditions. An example is shown in Fig. 4. In the asymmetric systems there are two bright arcs drifting in opposite directions and equatorward of those arcs weaker arcs drifting westward. The spacing between the arcs was even, 1–2 km, and the arc widths of the order of 500 m. Trondsen et al. suggested that a promising mechanism for the asymmetric parallel arc array was mode conversion of shear Alfvén waves to inertial Alfvén waves (Goertz, 1984) and that possibly field line resonances (Samson et al., 1996) were also involved. The mode conversion mechanism was the only mechanism discussed that could explain the asymmetry. Mode conversion can take place when the latitudinal scale size of the Alfvén waves is of the order of several electron inertia lengths, $\lambda_e = (m_e/\mu_0 ne^2)^{1/2}$ or less, where n is the electron density. Trondsen et al. (1997) compared the observed arc spacing mapped along the field line and the electron inertia length using an electron density profile taken from Borovsky (1993). They found that the two height profiles crossed at 2–3 R_E, and thus this was the likely altitude for the mode conversion.

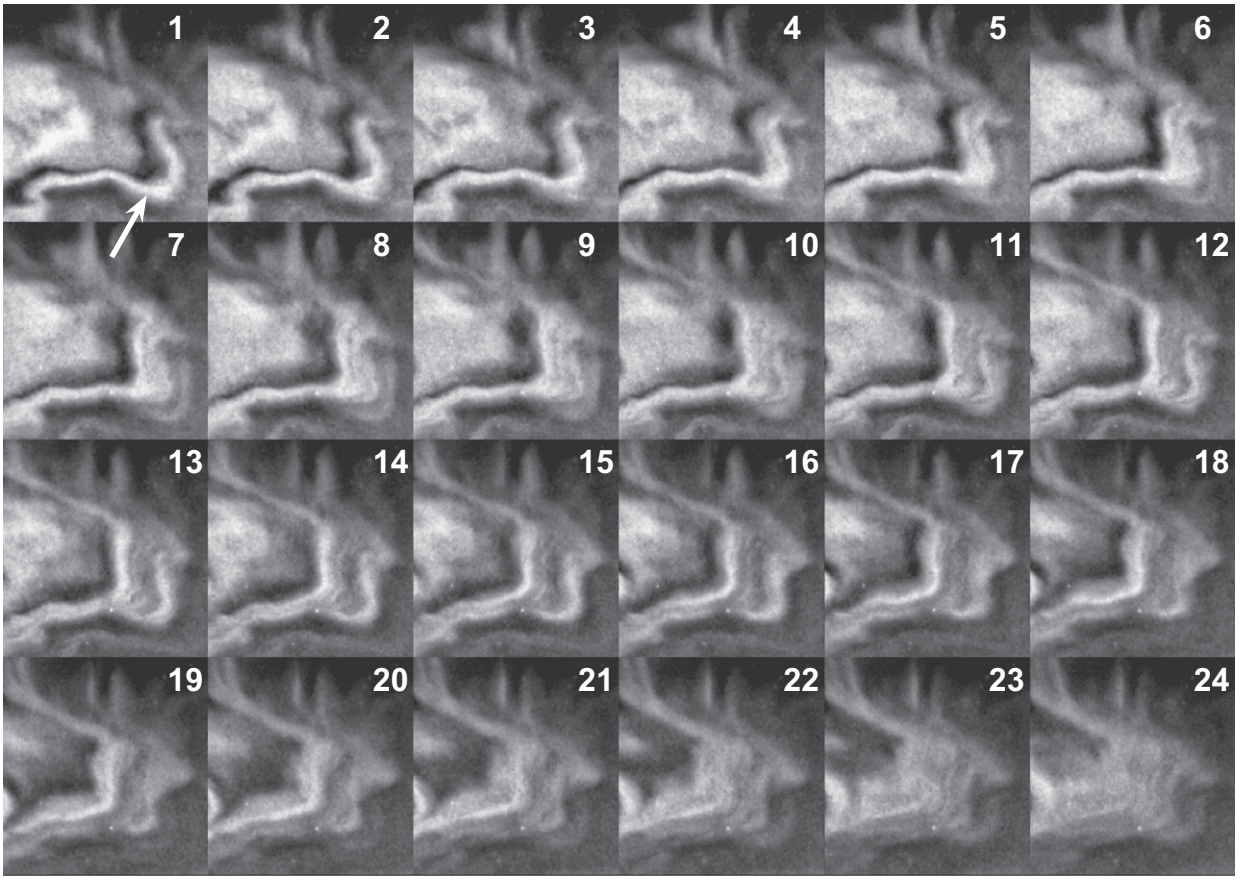

Fig. 3. Image sequence showing cascading of an initial arc into multiple arcs. The time between each frame is 20 ms and the whole sequence 0.5 s. Each frame shows an area of 11.7 × 11.1 km at 100 km altitude. The feature that is seen to cascade is indicated by an arrow in Image 1 (from Semeter and Blixt, 2006). Reproduced by permission of American Geophysical Union.

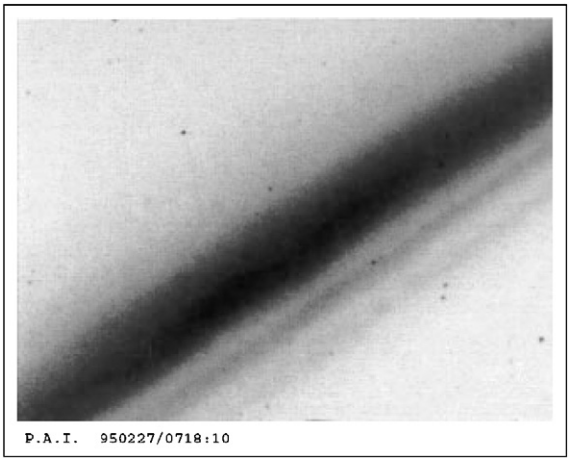

Fig. 4. Asymmetric multiple arc system with two weaker secondary arcs equatorward of the main arc. Such a configuration is fairly common in active auroras. The image was recorded in white light and the field of view was $7.4 \times 5.5^{\circ}$. The orientation of the figure is such that equatorward is to the right of the main arc (from Trondsen et al, 1997). Reproduced by permission of American Geophysical Union.

Even if mode conversion of Alfvén waves at a relatively low altitude seems to offer a promising explanation for such multiple arc systems, it is actually not known if there is a connection between Alfvén waves and narrow optical arcs in general. As noted by Stasiewicz et al. (2000) too few simultaneous observations of Alfvén waves and optical aurora exist. Alfvén waves can only accelerate auroral electrons up to about 1 keV and the statistics and modelling from FAST points to a width of Alfvén wave generated arcs of about 1 km (Chaston et al., 2003). Another important point is that Alfvén waves in the nightside, where most of the arc width studies have been carried out, are most frequently observed in the downward current region and not in regions with inverted Vs. In particular, the structures with the smallest scales are connected with the downward current region (Stasiewicz et al., 2000). For the evening side this means the equatorward part of the auroral oval, region 2, the region of diffuse aurora. The simulations by Streltsov and Lotko (2004) also showed the finest scales in field-aligned currents in the large-scale downward current region.

According to Stenbaek-Nielsen et al. (1999) most of the narrow arcs of Maggs and Davis (1968) appeared against a background of diffuse aurora. Could it in fact be so that isolated narrow arcs are a diffuse aurora phenomenon? How often are really narrow arcs isolated or is it more common that they appear in a set of multiple arcs? To evaluate different mechanisms we must have more complete information about the narrow arcs. For each arc not only the width is needed, but also the length of the arc and the temporal development including lifetime and speed and direction of motion, and, of course, intensity. It is also necessary to record its larger morphological context, for example if the arc appears against a wider diffuse arc, a generally diffuse background, in a region of large-scale upward or downward currents, and its relation to substorm activity. Such statistics can then be compared to the corresponding satellite data.

3.2. Auroral curls and filaments

Active arcs undergo deformation on different scales. Hallinan and Davis (1970) classified these deformations into spirals, folds, and curls. Of these, the curls are the smallest ones and the ones of relevance when discussing small-scale structures. Curls usually form vortex streets along arcs. According to Hallinan (1976) the typical spacing between curls along an arc is 8 km, they exist for a few seconds and move along the arc with a velocity of 10–20 km/s. Curls are wound counter clockwise when viewed antiparallel to the Earth's magnetic field and they are irreversible, that is, unlike spirals they do not unwind. When viewed from the side curls appear as rays. Hallinan and Davis (1970) attributed the curls to a Kelvin–Helmholtz instability. They proposed that curls are due to a sheet of negative charge. $\mathbf{E} \times \mathbf{B}$ drift surrounding the sheet gives rise to a velocity shear and to curl formation, the sense of which agrees with the counter clockwise direction.

Trondsen and Cogger (1998) used the PAI to study the detailed morphology of curls. Their study gave the same size range as the study by Hallinan and Davis (1970), 1–9 km, but it had a larger proportion of small curls. The preferred spacing between curls was 3 km, the typical size of one curl 1×2 km, the preferred area 0.5 km^2, and the preferred lifetime 0.25–0.75 s. No explanation for the size distribution difference as compared to the results by Hallinan and Davis (1970) is given, but the PAI is a much more sensitive and linear instrument than the image orthicon system used by Hallinan and Davis and the sample size was bigger, 415, while Hallinan and Davis had 104. Filaments connecting the curls were extremely thin, 100–300 m. The relation of arc width to wavelength was found to agree with a Kelvin–Helmholtz instability assumed to result from the $\mathbf{E} \times \mathbf{B}$ drift as proposed by Hallinan. Some examples of curl systems from Trondsen and Cogger (1998) are shown in Fig. 5, panel a, and the evolution of a curl system is shown in Fig. 5, panel b. The field of view of each frame was about 13.5×10.1 km. In Fig. 6, taken from Vogt et al. (1999) each frame shows a larger area, approximately 40×30 km. Here we see a sequence of images of several parallel curl systems with a temporal resolution of 1 s.

Haerendel et al. (1996) remarked that too few observations of the growth of curls exist. Vogt et al. (1999) studied the evolution of a curl system and could observe both the velocity shear and the curl growth rate. They concluded that the observed growth rate was bigger than what could be explained by the observed velocity shear and that the discrepancy could be resolved by an Alfvén wave of sufficiently large amplitude. As a result of their study they suggested that future models of the evolution of small-scale auroral phenomena must take auroral acceleration mechanisms and transient processes into account.

A confirmation of this suggestion was given by Hallinan et al. (2001). The rocket AMICIST passed multiple

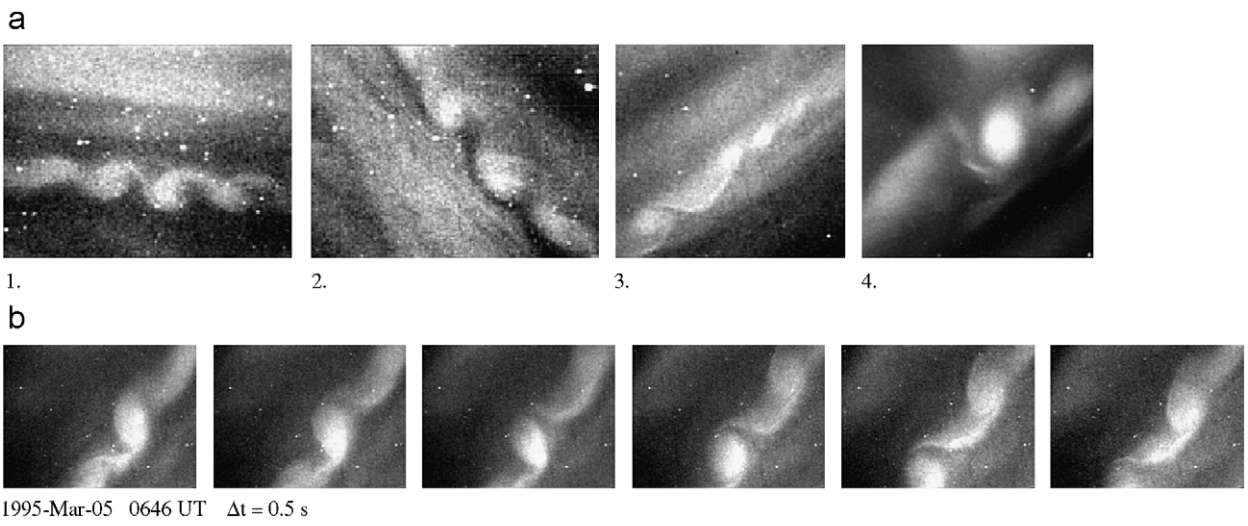

Fig. 5. Curl systems. (a) Four different examples of curl systems. (b) The temporal evolution of a curl system. The time between the frames is 0.5 s. The area shown in each frame is 13.5 × 10.1 km at an altitude of 105 km (adapted from Trondsen and Cogger, 1998). Reproduced by permission of American Geophysical Union.

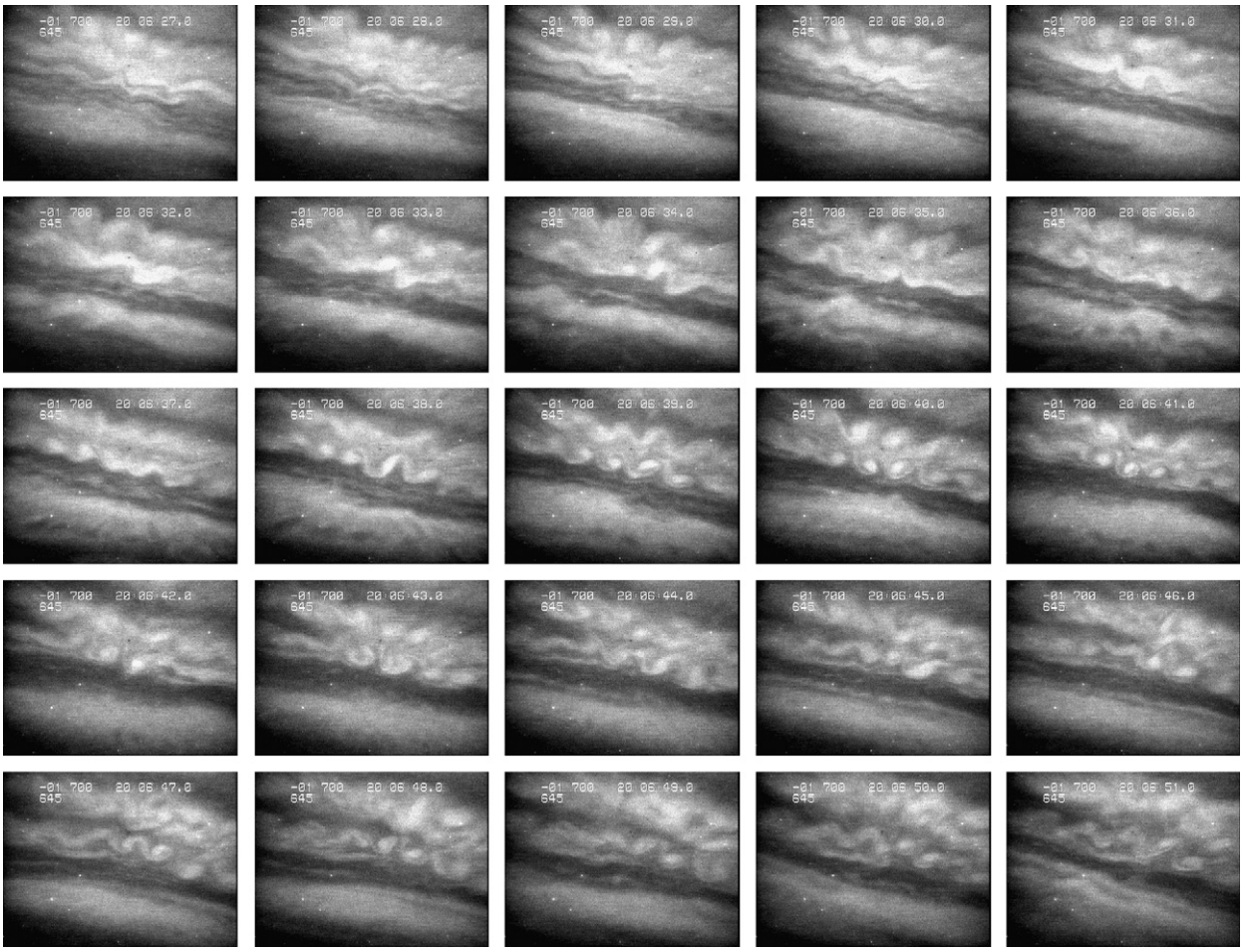

Fig. 6. Parallel curl systems. Each image shows an area of approximately 40 × 30 km and the temporal resolution is 1 s. From such images shear velocities and curl growth rates were determined (from Vogt et al., 1999). Reproduced by permission of American Geophysical Union.

rayed arcs that were also recorded by two intensified CCD cameras, one all-sky and one narrow angle. The particle measurements agreed well with the traditional model of acceleration in a quasi-static parallel electric field. The bulk motion of the rays agreed with what should be expected from the electric field at high altitude that was derived from the rocked measurements. Alfvén waves detected by the rocket were clearly related to the passage of a Kelvin–Helmholtz vortex street. A somewhat surprising observation was that the lower border of the aurora was higher than expected from the measured electron energies. If the lower border of the aurora was taken to be at an altitude of 130 km excellent matching was achieved between the relative optical intensity measured from the ground and the primary particle energy flux measured by the rocket. However, a lower border at 130 km implies primary particles with energy of 1–2 keV, while the measured electron distribution peaked at 4–5 keV. The reason for this discrepancy was not understood.

Hallinan and Davis (1970) could show that auroral curls looked like rays when viewed from the side. Ivchenko et al. (2005) found that the reverse is not always true. Some rays are clearly not curls. They used three sensitive imagers and the HiTIES spectrograph at Spitsbergen. The two intensified CCD imagers Odin (Blixt et al., 2005a) and the SIF imager (McWhirter et al., 2003) had a separation of 7.2 km and were operated at 25 frames per second with long-pass filters accepting wavelengths greater than 645 nm. An Andor iXon EMCCD camera was operated at 1–4 frames per second with a narrow-band filter at 724.5 nm and a field of view of $9 \times 9^{\circ}$. The luminosity in curls was found to have a small vertical extent centred around 120 km altitude, while there were also very tall rays with luminosity in the altitude range 130–400 km that were not curls. The lack of low-energy electrons in curls point to an electrostatic instability.

The term auroral filament is used for luminous structures in the aurora with a very small extent perpendicular to the magnetic field. The term is quite general and not part of any official optical auroral classification. Auroral filaments may be regarded as the smallest element in an active auroral arc.

Auroral filaments have been seen as narrow intense features embedded in the less intense background of an arc. Lanchester et al. (1997) observed an arc with EISCAT, photometer, and intensified TV cameras, and then modelled the arc using a Maxwellian with peak energy of 8 keV for the background arc and a Gaussian (monoenergetic) beam of 22 keV for the filament. The width of the filament was concluded to be 100 m and the energy flux in the filament more than 500 mW/m^2. Dahlgren et al. (2008) could confirm this result with ASK and HiTIES. Some

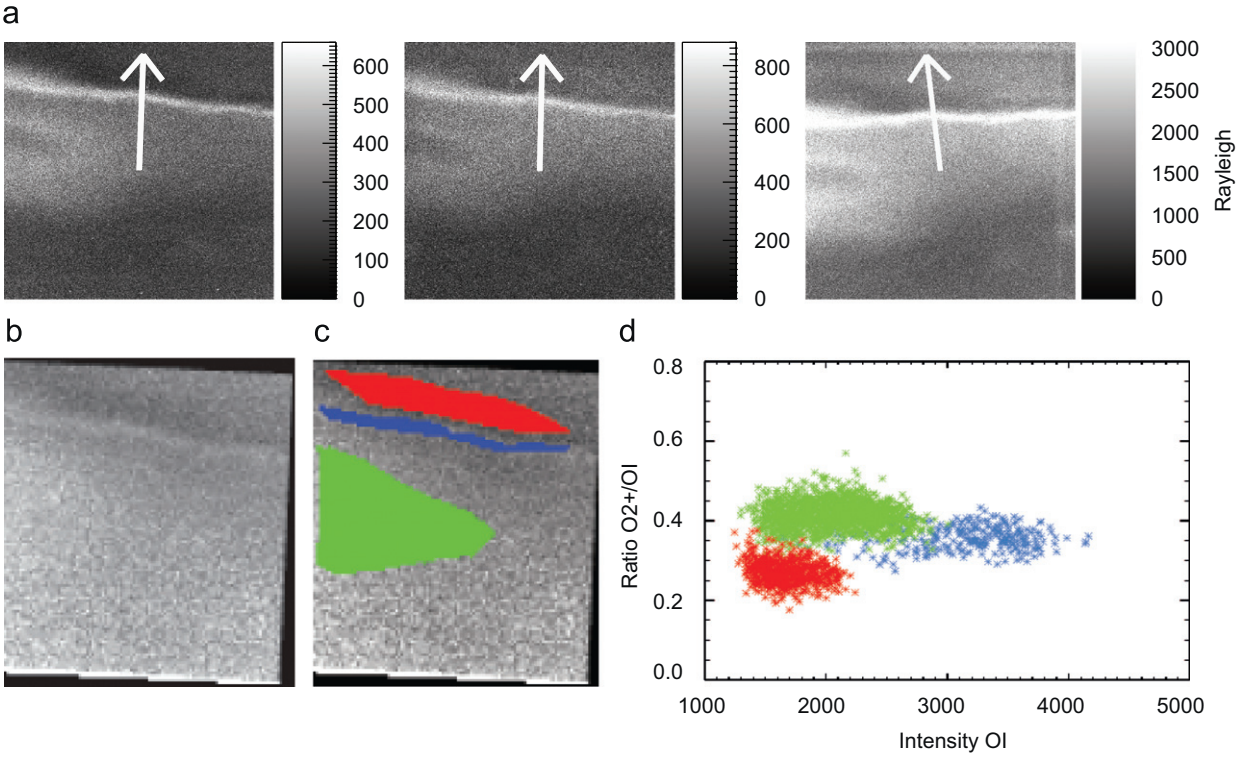

Fig. 7. A bright auroral filament recorded by ASK. These data show that the bright filament was caused by primary electrons of a higher energy than the wider background arc. (a) Simultaneous images obtained by the three ASK cameras showing the intensities of O_2^+, O^+, and OI. (b) Intensity ratio O_2^+/OI. A high ratio corresponds to a high characteristic energy. (c) In this plot three different regions with different intensity levels are marked. The bright filament is blue, a darker region north of the filament is red, and less intense aurora equatorward of the filament is green. (d) Intensity ratio as a function of the OI intensity for all pixels within the regions marked in panel c. The narrow arc, blue, corresponded to a higher characteristic energy than the adjacent region marked by red (from Dahlgren et al., 2008).

Fig. 8. EISCAT field of view compared to the width of a filament. The field of view is 38 × 28 km; north is to the right and east to the top. The circle gives the field of view of both EISCAT and a photometer. Its diameter is about 900 m. Neither of these instruments can thus directly resolve the 100 m wide filament (from Lanchester et al., 1997). Reproduced by permission of American Geophysical Union.

auroral filaments were caused by high energy precipitation within a region of lower energy precipitation. ASK used 0.2 s exposure time in this case. The narrowest structures found were 200 m. ASK data from this event are shown in Fig. 7. Dahlgren et al. (2008) also found a bright fold that was caused by a higher particle flux compared to the surrounding regions, not higher energies.

The fine structure of the auroral forms is related to the same level of fine structure in the electrodynamics. Short-lived precipitation bursts give rise to very large but short-lived electric fields adjacent to the filaments (Lanchester et al., 1996, 1998). In a case studied by Lanchester et al. (1998) the electric field reached 600 mV/m and was directed into the bright filament, but still located adjacent to it. Fig. 8, from Lanchester et al. (1997), shows another case in which an auroral filament was much narrower than the field of view of EISCAT. In many types of measurements the resolution has been too poor to be able to detect this kind of spatial pattern. Without high-resolution optical measurements one might, for example, believe that the strong electric field is actually inside the aurora.

The precipitation causes build-up of electron density, temperature, and ionospheric conductivity, but the time constant for this is slower than many of the variations in the aurora (Lanchester et al., 1998). This was observed in a dynamic arc consisting of several filaments by Lanchester et al. (2001) with EISCAT and two cameras, including a 15 × 21 field of view intensified CCD camera (Frey et al., 1996a). The EISCAT experiment was designed to give a high temporal resolution. The event was modelled in two companion studies, a transport simulation by Lanchester et al. (2001) and a two-dimensional three-fluid simulation of the ionosphere–magnetosphere system by Zhu et al. (2001). In the simulation the initial perturbation was a pair of Alfvén waves. Observations of a very large and sudden electron temperature increase adjacent to an auroral filament could be explained by ohmic heating by a strong burst of field-aligned current reaching a peak value of 400 μA/m^2. To reach agreement with the observations the most intense field-aligned current had to be located immediately beside the optical arc. From the simulation it could not be determined if this current was upward or downward since heating will be produced in both cases, but to us it seems most likely that it was downward. Very strong and very localized currents were also found in the Freja data by Stasiewicz and Potemra (1998). The narrower the structure, the higher the current density. The highest current densities, 100–300 μA/m^2, appeared in current structures of subkilometer scales.

In summary, in a few studies a combination of a Kelvin–Helmholtz instability and acceleration in a quasi-static parallel electric field seems to explain the formation of curls quite successfully. More work is needed to determine to what extent this is generally true. The current of 400 μA/m^2, used in the modelling by Lanchester et al. (2001), is quite a strong current density for the ionosphere. What happens to this current at higher altitude? If such strong currents are a regular feature in connection with curl formation, there should be a statistical relationship to currents measured from satellites. Zhu et al. (2001) also noted that to study the deformation of a field-aligned current along an auroral arc a three-dimensional model is needed.

3.3. Auroral rays

In this section we discuss auroral rays that sometimes appear singly or more often in isolated bundles or more extended groups. Ray is one of the 12 basic auroral forms according to the widely used classification by Størmer (1955). We recall that Størmer divided the basic auroral forms into three groups, forms without ray structure, forms with ray structure, and flaming aurora. He listed five different forms with ray structure: (1) rayed arc, (2) rayed band, (3) drapery, (4) ray, and (5) corona. The term ray was used for all auroral forms with a comparatively long extent along the magnetic field and small horizontal extent in all directions perpendicular to the magnetic field. Rays may be short or long, narrow or broad. They may be stationary or move slowly. The length may vary rapidly. They can have different colours. Often the upper part is red or they are red all over. Størmer was particularly interested in rays in the sunlit atmosphere that can reach heights up to 1000 km. He also mentions divided rays that have an upper and a lower section separated by a darker space near the Earth's shadow. Certainly, a number of different mechanisms are needed to explain all the features of different rays.

In his summary of salient features of auroral structures Chamberlain (1961) notes that "Rayed structure may become exceedingly fine, probably as narrow as 0.1 km and perhaps even less for some of the short-lived (less than one second) structure".

One type of rays is the tall red ray, single beams of aurora with a very large vertical extent, from a lower border at 150–200 km up to as high as 600 km and the width between 1 and 10 km. The luminosity profile of the OI 630.0 nm emission is fairly constant. For a long time,

the mechanism behind these rays has been a mystery. It is difficult to imagine a mechanism in which precipitating electrons could give such an emission profile. Otto et al. (2003) applied the simulation model of Zhu et al. (2001) and could show that a filamentary current density of 600 $\mu A/m^2$ with a duration of 10 s could give enough energy to the ambient oxygen atoms to produce visible emissions. The mechanism requires that sufficient oxygen is present.

The rays studied in Spitsbergen by Ivchenko et al. (2005), mentioned in Section 3.2, had developed from a collection of thin and intense multiple arcs that broke into several thin rayed arcs in which the rays appeared to be independent. Thus the term "extended group of rays" may be more appropriate for the case than rayed arcs. The altitude range of 130–400 km point to primary electron energies from just a few eV and up to between 1 and 2 keV. Some of the rays had a diameter of only 200 m. The HiTIES spectrograph showed a very strong contribution from the OII 732 and 733 nm doublet. Based on the wide energy range of the primary particles and the small horizontal extent of the rays, it was concluded that they were caused by dispersive Alfvén waves.

Such dynamic rayed aurora is related to the NEIALs, which are measured by incoherent scatter radar. Using the two high-resolution imagers PAI and Odin together with the HiTIES spectrograph and the EISCAT Svalbard radar Blixt et al. (2005a, b) could show that dynamic rayed aurora appeared at the same time and place as NEIALs. A particularly convincing event was one in which the rays were viewed from two different sites 7 km apart. A necessary factor for the result was the high temporal and spatial resolution of the measurements. To resolve the enhanced radar echoes a time resolution of 0.2 s is required and the rays where they occur can be narrower than a few hundred meters perpendicular to the magnetic field (Grydeland et al., 2003). Recent measurements with the AMISR radar at Poker Flat, Alaska, with a resolution of 19 ms, together with a narrow field ICCD imager, showed that indeed the NEIALs were associated with dynamic aurora. They concluded that the source of the NEIAL was in the dark region adjacent to the bright aurora (Michell et al., 2008). Fig. 9 shows the returned power from the raw radar data with full temporal resolution together with the relative intensity of the aurora inside the radar beam. The NEIALs appear as very short-lived bursts in the 200–250 km height region.

Detailed measurements of the particle distribution in isolated auroral rays are rare, but they exist. The rocket AMICIST, previously discussed in Section 3.2, crossed a tall transient ray toward the end of its flight (Hallinan et al., 2001). The ray had a lower border of 170 ± 10 km and considerable height. The energy range of the primary electrons was 100–800 eV.

In the case of dynamic rayed aurora the most commonly discussed mechanism is electron acceleration by Alfvén waves. However, more detailed calculations are needed to show if this can really explain structures as tall as 130–400 km and as narrow as 200 m that were measured by Ivchenko et al. (2005). Neither a Maxwellian

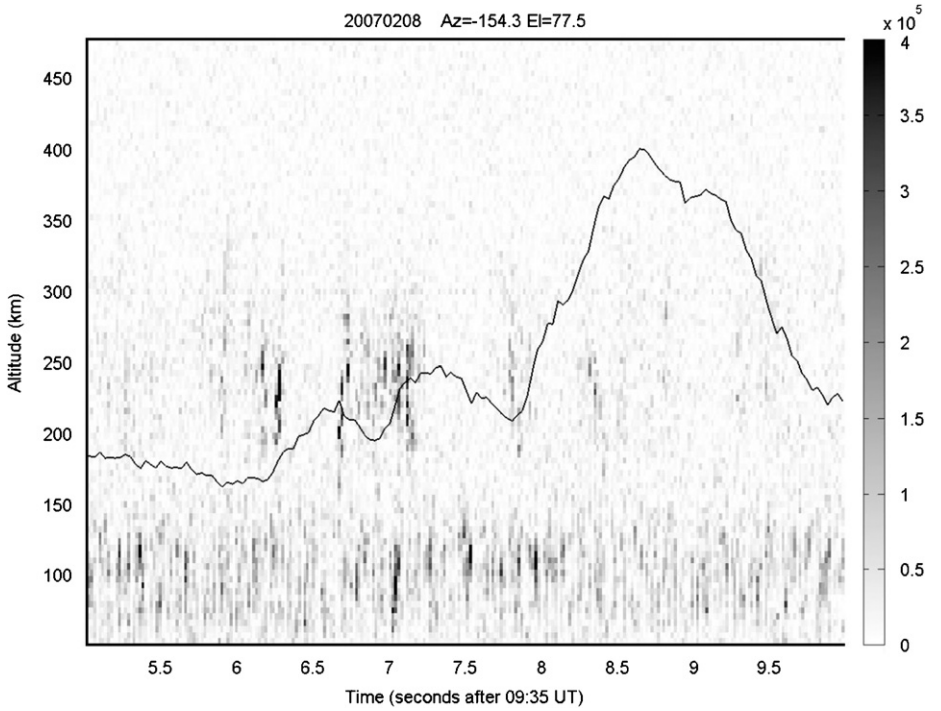

Fig. 9. NEIALs measured by AMISR. The figure shows the returned power from the raw radar data with full (19 ms) temporal resolution and the whole plot represents 5 s of data. The NEIALs appear as intense, very short-lived bursts from about 200 to 250 km. The solid line shows the relative intensity of the aurora inside the radar beam. The emission at 557.7 nm had been removed by a notch filter (from Michell et al., 2008).

nor a Gaussian initial electron distribution is able to produce light of such high vertical extent. For the tall single rays the heating of ambient oxygen by an intense filamentary current (Otto et al., 2003) is promising, but much more work is needed to establish if mechanisms of this type can explain all tall single rays. The mechanism creating the strong filamentary current needs to be found and it needs to be shown that enough oxygen is present.

A different type of mechanism for the creation of rays has been proposed by I. Kornilov and A. Safargaleev in a presentation at the 34th Annual European Meeting on Atmospheric studies by Optical Methods. A fast temporal variation of the characteristic energy and/or intensity of the primary particle flux could cause luminosity that appears as stationary to the human eye or to instruments with insufficient temporal resolution. Some auroral TV data supporting such a mechanism were presented.

3.4. Black aurora

Black auroras were originally defined as a lack of emission in well-defined regions within diffuse aurora or within regions that are intermediate between diffuse and discrete aurora (Røyrvik, 1976; Davis, 1978a). The widths of black aurora structures are typically 500 m (Trondsen and Cogger, 1997; Kimball and Hallinan, 1998), and black aurora is thus a fine structure phenomenon. Narrow black streaks are also observed to appear in active auroral arcs. Such streaks are also sometimes called black aurora (Marklund et al., 2001) although they do not conform to the original definition of black aurora.

Trondsen and Cogger (1997) carried out a study of the morphology of black aurora using PAI. They measured the spatial and temporal characteristics of different forms in the evening sector diffuse auroral oval. These forms were eastward travelling black objects, black streaming, black arcs, and vortex street formation in black arcs. Black objects had sizes of 1–2 km^2 and drifted eastward with a velocity of 1–1.5 km/s, more or less maintaining their shape. Black arcs had a preferred thickness of 400–500 m and were longer than the field of view of the camera. Black arcs were frequently multiple with a preferred spacing of 1 km. These black arcs were fairly stable, in many cases observed for several minutes. In addition, there were more transient black arcs that had a width of less than 100 m. Black vortex streets were relatively rare. They were similar to curls, except that they had a clockwise sense of rotation. When determining the sizes of the black features Trondsen and Cogger (1997) assumed an altitude of 105 km, the assumed altitude of the surrounding diffuse aurora.

Two types of generation mechanisms for black aurora have been proposed:

1. A mechanism in the ionosphere in which downward field-aligned currents associated with a positive space charge pull cold electrons out of the topside ionosphere (Marklund et al., 2001 and references therein, Trondsen and Cogger, 1997).
2. A mechanism in the magnetosphere that locally decreases the strong pitch angle diffusion into the loss cone (Kimball and Hallinan, 1998; Peticolas et al., 2002; Blixt and Kosch, 2004; Gustavsson et al., 2008).

It is probable that different mechanisms cause different types of black auroras. The downward FAC mechanism has above all been associated with black vortex streets.

Most ground-based optical measurements of black aurora favour mechanisms of the second type, mechanisms involving pitch angle diffusion. Blixt and Kosch (2004) used the Odin imager and EISCAT to study non-sheared black aurora. The EISCAT data showed no ionospheric density depletion, and thus they concluded that this black aurora was not related to a downward current. One of the black arcs in this study is shown in Fig. 10. Blixt et al. (2005b) then investigated the drift of black patches. In seven of the eight events studied the patches drifted eastward with velocities of 1.5–4 km/s. The black structures had a higher drift velocity than the $\mathbf{E} \times \mathbf{B}$ plasma flow measured by EISCAT. This speaks against an ionospheric origin. From EISCAT electron density profiles the particle energy of the background precipitation was derived and a correlation between the particle energy and the drift velocity of the black structures was found. The drift velocities of the patches corresponded to gradient-B curvature drift of 10–50 keV particles, while the characteristic energies of the background population derived from EISCAT were 2–11 keV. This difference could be explained if the decrease in pitch angle scattering is related to particles with higher energies. In a recent paper Gustavsson et al. (2008) report results from simultaneous incoherent scatter and advanced optical measurements of an un-sheared black aurora. They performed absolute measurements of the reduction of the prompt emissions at 427.8 and 844.6 nm in the black structures. Using the electron density profile obtained by EISCAT, they estimated the spectrum responsible for the diffuse aurora surrounding the black aurora. With this spectrum as input they modelled the light reduction for the two competing

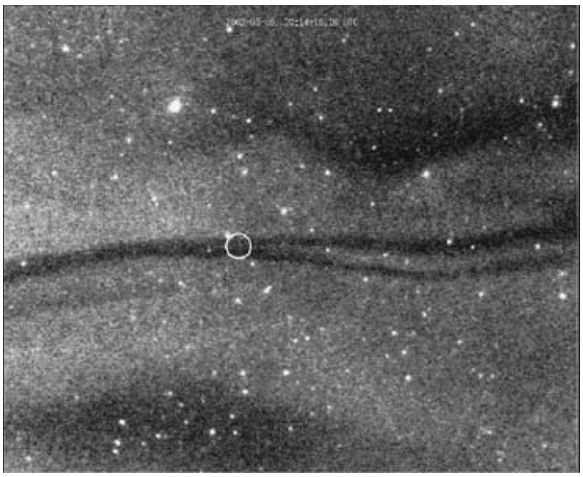

Fig. 10. Black arc. This black arc was recorded by the Odin imager above EISCAT. The circle shows the diameter of the radar beam. The width of the arc went from 2 to 1 km. No density depletion was detected by EISCAT (from Blixt and Kosch, 2004). Reproduced by permission of American Geophysical Union.

mechanisms and could show that the relative reduction of the two emissions was only compatible with suppression of pitch angle diffusion.

The first near conjugate optical and particle measurements of black aurora were reported by Peticolas et al. (2002). The particle measurements were carried out by FAST and the optical imagers were placed on an aircraft. They studied a 6.5 km wide black arc with curls in a diffuse background. FAST measured double loss cone distributions in the black aurora and single loss cone distributions outside. Thus, the black arc was most likely due to blocking of the pitch angle diffusion at energies above 2 keV. FAST data were searched for signatures that would be expected for mechanism 1: significant electric fields, positive space charge, upward fluxes of electrons, deceleration of downward electrons, but none of these were found. It was suggested that the pitch angle diffusion in the diffuse aurora was due to electron cyclotron harmonic waves and whistler-mode upper band chorus waves, and that the chorus waves were suppressed in the black aurora. It is somewhat surprising that the black aurora exhibited curls. A common explanation of black vortex streets is that they are due to sheets of positive space charge, but this was not observed.

With the Reimei satellite the first exactly simultaneous measurements of optical black aurora and particles were carried out and they gave a similar result (Obuchi et al., 2006). The black aurora clearly corresponded to a region with a double loss cone, while the surrounding diffuse aurora had a single loss cone. In addition, energy dispersed precipitating electrons were observed.

Mechanism 1, upward acceleration of electrons certainly exists. The previously mentioned simulation by Streltsov (2007) also showed that when there are two oppositely directed strong current sheets a narrow and very intense downward current can form in the conductivity gradient between the original upward and downward current. The formation of this intense downward current is associated with the formation of a highly localized downward potential drop. However, there are no unambiguous measurements of the corresponding optical signature. There is also a need to agree on the nomenclature. Gustavsson et al. (2008) used the term "sheared black auroras" for auroras caused by downward electric fields. Future research will show if this is a relevant name.

4. Conclusions and the road ahead

Fine-scale structures, both temporal and spatial, are common in most auroral forms, both discrete and diffuse. Measuring these puts high demands on the instrumentation. So far it has been possible to measure some, but not all properties of fine-scale aurora. Ground-based optical instruments give the best resolution, both in time and space. In this paper, we have discussed the available instrumentation for fine-scale measurements and some specific types of small-scale aurora, narrow arcs, curls and filamentary aurora, auroral rays, and black aurora.

As shown in Section 3 there are still many unanswered questions regarding formation mechanisms of different fine-scale structures. In fact, our conclusion is that there is no small-scale structure for which the mechanism is completely understood. It is also not understood how and how much they couple back to the magnetosphere. To make progress in the field we need to carry out more detailed observations, improve auroral models, and improve modelling of magnetosphere–ionosphere processes. The recent developments in the field of optical instrumentation hold promises for greatly improved observations in the near future.

Borovsky (1993) suggests nine ground-based observations that should be carried out to resolve the problem of formation of thin auroral arcs. The items on this list are

1. Measuring the thickness of larger-scale arc structures.
2. Correlating fine-scale arcs with larger arc structures.
3. Measuring the height of fine-scale arcs.
4. Measuring optical emission line ratios.
5. Keeping separate statistics for breakup arcs and quiet arcs.
6. Correlating all-sky camera images with data from geosynchronous satellites.
7. Following Alfvén waves transmitting between conjugate arcs.
8. Measuring auroral-arc temporal fluctuations.
9. Correlating arc thicknesses with other arc parameters.

This list is still highly relevant and can serve as a basis for a revised list of recommended measurements.

1. Establish sizes and distribution of sizes of each auroral form. Since different mechanisms lead to different sizes, this is vital information. For narrow arcs it is desirable also to measure the length, even if this is in practice a very complicated task.
2. Measure additional properties of each auroral form. For each event the absolute intensity should also be measured, as well as the temporal behaviour including lifetime and horizontal drift velocity, so that the relationships between the different properties of the small-scale structures can be established. For example, it is of interest to determine how well the relationship between intensity and width agrees with the statistics for Alfvén wave generated arcs presented by Chaston et al. (2003).
3. Measure the large-scale context of the small-scale structures. Does the structure appear in a region of diffuse aurora or discrete aurora? Is it a part of a weaker wider arc? Does it appear during a substorm or during magnetically quiet times? Is the large-scale current upward or downward. What is the magnetic local time? Of course, it has very important implications for the mechanism of narrow arcs if it is indeed true that they mainly appear in the region of diffuse aurora (Stenbaek-Nielsen et al., 1999). Do the regions of downward large-scale current contain small-scale structures corresponding to the simulations by Streltsov and Lotko (2004)? What are the distributions of different kinds of black auroras? The list of questions here can be made long. For the study of

cross scale coupling, multiscale observations are absolutely necessary.

4. Measure the vertical luminosity distribution of small-scale structures including their temporal development. The vertical luminosity distribution contains information about the primary electrons as well as about local processes in the ionosphere leading to light production. Borovsky (1993) discussed the practical difficulties in performing such measurements for small-scale structures. With modern optical instrumentation, the possibilities for such measurements are much improved. A good example is the study of curls and rays by Ivchenko et al. (2005).
5. Optical emission line ratio measurements. Thanks to the superior light-gathering power of some of the modern imagers it is now possible to do line ratio measurements using prompt emissions, and thus this method has become much more useful. This is one of the important ideas behind the ASK instrument. The O_2^+ first negative band at 562.0 nm comes from the E region and the O emission at 777.4 nm from the both the E and the F region. Measurements of ratios of prompt lines make it possible to draw conclusions about the temporal evolution of the primary particle distribution. Furthermore, this can now be done for several points simultaneously, since each pixel can work as a photometer.

We would like to stress that measurements of optical small-scale structures need to be carried out in conjunction with other measurements. In this paper there are many examples of results that have been obtained by combining optical data and EISCAT data and where both have been essential for the interpretation of the other. There is also a shortage of optical measurements of small-scale structures in conjunction with particle and field measurements in space. Even if good conjunctions with satellites are rare, as discussed in Section 2.4, opportunities for such measurements should be taken advantage of. Sounding rockets offer the best possibility to carry out detailed small-scale particle and field measurements correlated with detailed optical measurements. In order to understand the relation between the small-scale structures and meso-scale and global-scale aurora, high-resolution measurements with a small field of view should be carried out together with measurements covering a larger part of the aurora. There is a continuous need for imagers viewing the aurora from space, since this is the best way to get the global overview.

To avoid confusion the classification of small-scale structures should be revisited. This could be done as a collaboration between scientists and groups working in the field.

To interpret the data concerning small-scale aurora it is necessary to improve models and analysis methods. Many terms that can be dropped when treating large- and medium-scale processes need to be retained. Frequently time-dependent models are needed and it is necessary to deal with details of collisions, ion chemistry, composition of the atmosphere, and measurements in which the structures do not fill the instrument fields of view.

A very general question is at what height the small-scale structuring is initiated. For bright, rayed auroral forms it has been concluded that they cannot map to the outer magnetosphere, but that they are most likely imposed at altitudes of 1–3 R_E (Galperin, 2002). In contrast, for fine structure that is due to modulation of pitch angle diffusion into the loss cone, such as non-sheared black auroras, the source may well be located much further out, perhaps even in the equatorial plane. If the narrow arcs studied by Davis and Hicks (1964) actually appeared against a diffuse aurora background, these arcs perhaps also map far out into the magnetosphere.

It will not be easy to understand the different small-scale auroral structures. But the tools to make progress are now available, powerful imagers and computers. Work towards this understanding is likely to generate a lot of knowledge about our upper atmosphere and about magnetosphere-ionosphere coupling.

Acknowledgements

This review was initiated as a part of the activities within IPY Cluster 63, Heliosphere Impact on Geospace. The research was supported by the Nordic Council of Ministers through grant 087043-60105, Network for Groundbased Optical Auroral Research in the Arctic Region and by the Swedish Research Council.

References

Akasofu, S.-I., 1968. Polar and Magnetospheric Substorms. D.Reidel Publ., Dordrecht, Holland.

Akasofu, S.-I., 2007. Exploring the Secrets of the Aurora, second ed. Astrophysics and Space Science Library 346, Springer.

Amm, O., Donovan, E.F., Frey, H., Lester, M., Nakamura, R., Wild, J.A., Aikio, A., Dunlop, M., Kauristie, K., Marchaudon, A., McCrea, I.W., Opgenoorth, H.-J., Strømme, A., 2005. Coordinated studies of the geospace environment using Cluster, satellite and ground-based data: an interim review. Annales Geophysicae 23, 2129–2170.

Anger, C.D., Babey, S.K., Broadfoot, A.L., Brown, R.G., Cogger, L.L., Gattinger, R., Haslett, J.W., King, R.A., McEwen, D.J., Murphree, J.S., Richardson, E.H., Sandel, B.R., Smith, K., Vallance Jones, A., 1987. An ultraviolet auroral imager for the viking spacecraft. Geophysical Research Letters 14, 387–390.

Asamura, K., Tsujita, D., Tanaka, H., Saito, Y., Mukai, T., Hirahara, M., 2003. Auroral particle instrument onboard the INDEX satellite. Advances in Space Research 32 (3), 375–378.

Ashrafi, M., 2007. ASK: Auroral structure and kinetics in action. Astronomy and Geophysics 48 (4), 35–37.

Baker, D.J., Romick, G.J., 1976. The Rayleigh interpretation of the unit in terms of column emission rate or apparent radiance expressed in SI units. Applied Optics 15, 1966–1968.

Blixt, E.M., Kosch, M.J., 2004. Coordinated optical and EISCAT observations of black aurora. Geophysical Research Letters 31, 6813.

Blixt, E.M., Grydeland, T., Ivchenko, N., Hagfors, T., La Hoz, C., Lanchester, B.S., Løvhaug, U.P., Trondsen, T.S., 2005a. Dynamic rayed aurora and enhanced ion-acoustic radar echoes. Annales Geophysicae 23, 3–11.

Blixt, E.M., Kosch, M.J., Semeter, J., 2005b. Relative drift between black aurora and the ionospheric plasma. Annales Geophysicae 23, 1611–1621.

Borovsky, J.E., 1993. Auroral arc thicknesses as predicted by various theories. Journal of Geophysical Research 98, 6101–6138.

Borovsky, J.E., Suszcynsky, D.M., Buchwald, M.I., DeHaven, H.V., 1991. Measuring the thickness of auroral curtains. Arctic 44, 231–238.

Brändström, U., 2003. The Auroral large imaging system—design, operation and scientific results. Ph.D. Thesis, Swedish Institute of Space Physics, Kiruna, Sweden, October 2003. IRF Scientific Report 279, ISBN:91-7305-405-4.

Chakrabarti, S., Pallamraju, D., Baumgardner, J., Vaillancourt, J., 2001. HiTIES: a high throughput imaging echelle spectrograph for

ground-based visible airglow and auroral studies. Journal of Geophysical Research 106, 30337–30348.
Chamberlain, J.W., 1961. Physics of the Aurora and Airglow. Academic Press, New York Original publication. Reprint edition American Geophysical Union, 1995.
Chaston, C.C., Peticolas, L.M., Bonnell, J.W., Carlson, C.W., Ergun, R.E., McFadden, J.P., Strangeway, R.J., 2003. Width and brightness of auroral arcs driven by inertial Alfven waves. Journal of Geophysical Research 108 SIA 17-1, CiteID 1091.
Chernouss, S., Sandahl, I., 2008. Comparison and significance of auroral studies during the Swedish and Russian bilateral expedition to Spitsbergen in 1899–1900. Annales Geophysicae 26, 1127–1140.
Chmyrev, V.M., Marchenko, V.A., Pokhotelov, O.A., Shukla, P.K., Stenflo, L., Streltsov, A.V., 1992. The development of discrete active auroral forms. IEEE Transactions on Plasma Science 20, 764–769.
Christensen, A.B., Paxton, L.J., Avery, S., Craven, J., Crowley, G., Humm, D.C., Kil, H., Meier, R.R., Meng, C.-I., Morrison, D., Ogorzalek, B.S., Straus, P., Strickland, D.J., Swenson, R.M., Walterscheid, R.L., Wolven, B., Zhang, Y., 2003. Initial observations with the Global Ultraviolet Imager (GUVI) in the NASA TIMED satellite mission. Journal of Geophysical Research (Space Physics) 108 (A12), 1451.
Dahlgren, H., Ivchenko, N., Sullivan, J.M., Lanchester, B.S., Marklund, D., Whiter, K., 2008. Morphology and dynamics of aurora at fine scale: first results from the ASK instrument. Annales Geophysicae 26, 1041–1048.
Donovan, E., Mende, S., Jackel, B., Frey, H., Syrjäsuo, M., Voronkov, I., Trondsen, T., Peticolas, L., Angelopoulos, V., Harris, S., Greffen, M., Connors, M., 2006. The THEMIS all-sky imaging array—system design and initial results from the prototype imager. Journal of Atmospheric and Terrestrial Physics 68, 1472–1487.
Davis, T.N., 1978a. Observed microstructure of auroral forms. Journal of Geomagnetism and Geoelectricity 30, 371–380.
Davis, T.N., 1978b. Observed characteristics of auroral forms. Space Science Reviews 22, 77–113.
Davis, T.N., Hicks, G.T., 1964. Television cinematography of auroras and preliminary measurements of auroral velocities. Journal of Geophysical Research 69, 1931–1932.
Feldstein, Y.I., 1963. Some aspects of the auroral morphology and geomagnetic disturbances in the high latitudes. Geomagnetism and Aeronomy 3, 227–239 (in Russian).
Frank, L.A., Sigwarth, J.B., Craven, J.D., Cravens, J.P., Dolan, J.S., Dvorsky, M.R., Hardebeck, P.K., Harvey, J.D., Muller, D., 1995. The visible imaging system (VIS) for the polar spacecraft, (Reprinted in The Global Geospace Mission ed. By C.T, Russell, Kluwer Academic Publishers, 1995). Space Science Reviews 71, 297–328.
Frey, H.U., Haerendel, G., Buchert, S., Lanchester, B.S., 1996a. Auroral-arc splitting by intrusion of a new convection channel. Annales Geophysicae 14, 1257–1264.
Frey, S., Frey, H.U., Carr, D.J., Bauer, O.H., Haerendel, G., 1996b. Auroral emission profiles extracted from three-dimensionally reconstructed arcs. Journal of Geophysical Research 101, 21731–21741.
Galperin, Y.I., 2002. Multiple scales in auroral plasmas. Journal of Atmospheric and Solar-Terrestrial Physics 64, 211–229.
Goertz, C.K., 1984. Kinetic Alfvén waves on auroral field lines. Planetary and Space Science 32, 1387–1392.
Grydeland, T., La Hoz, C., Hagfors, T., Blixt, E.M., Saito, S., Strømme, A., Brekke, A., 2003. Interferometric observations of filamentary structures associated with plasma instability in the auroral ionosphere. Geophysical Research Letters 30, 71–74.
Gustavsson, B., 1998. Tomographic inversion for ALIS noise and resolution. Journal of Geophysical Research 103, 26621–26632.
Gustavsson, B., 2000. Three dimensional imaging of aurora and airglow. Ph.D. Thesis, Swedish Institute of Space Physics, Kiruna, Sweden, September 2000. IRF Scientific Report 267, ISBN:91-7191-878-7.
Gustavsson, B., Kosch, M.J., Senior, A., Kavanagh, A.J., Brändström, B.U.E., Blixt, E.M., 2008. Combined EISCAT radar and optical multi-spectral and tomographic observations of black aurora. Journal of Geophysical Research 113, A06308, doi:10.1029/2007JA012999.
Haerendel, G., Olipitz, B.U., Buchert, S., Bauer, O.H., Rieger, E., La Hoz, C., 1996. Optical and radar observations of auroral arcs with emphasis on small-scale structures. Journal of Atmospheric and Terrestrial Physics 58, 71–83.
Hallinan, T.J., 1976. Auroral spirals 2. Theory. Journal of Geophysical Research 81, 3959–3965.
Hallinan, T.J., Davis, T.N., 1970. Small-scale auroral arc distortions. Planetary and Space Science 18, 1735–1744.
Hallinan, T.J., Kimball, J., Stenbaek-Nielsen, H.C., Lynch, K., Arnoldy, R., Bonnell, J., Kintner, P., 2001. Relation between optical emissions, particles, electric fields, and Alfvén waves in a multiple rayed arc. Journal of Geophysical Research 106, 15445–15454.
Hunten, D.M., Roach, F.E., Chamberlain, J.W., 1956. A photometric unit for the airglow and aurora. Journal of Atmospheric and Terrestrial Physics 8, 345–346.
Ivchenko, N., Blixt, E.M., Lanchester, B.S., 2005. Multispectral observations of auroral rays and curls. Geophysical Research Letters 32, 18106, L18106.
Kaila, K.U., Holma, H.J., 2000. Absolute calibration of photometer. Physics and Chemistry of the Earth B (25), 467–470.
Kimball, J., Hallinan, T.J., 1998. A morphological study of black vortex streets. Journal of Geophysical Research 103, 14683–14695.
Knudsen, D.J., Donovan, E.F., Cogger, L.L., Jackel, B., Shaw, W.D., 2001. Width and structure of mesoscale optical auroral arcs. Geophysical Research Letters 28, 705–708.
Korosheva, O.V., 1962. Daily drift of continuous auroral ring. Geomagnetism and Aeronomy 2, 839–850.
Kosch, M.J., Hagfors, T., Nielsen, E., 1998. A new digital all-sky imager experiment for optical auroral studies in conjunction with the Scandinavian twin auroral radar experiment. Review of Scientific Instruments 69, 578–584.
Lanchester, B.S., Kaila, K., McCrea, I.W., 1996. Relationship between large horizontal electric fields and auroral arc elements. Journal of Geophysical Research 101, 5075–5084.
Lanchester, B.S., Rees, M.H., Lummerzheim, D., Otto, A., Frey, H.U., Kaila, K.U., 1997. Large fluxes of auroral electrons in filaments of 100 m width. Journal of Geophysical Research 102, 9741–9748.
Lanchester, B.S., Rees, M.H., Sedgemore, K.J.F., Palmer, J.R., Frey, H.U., Kaila, K.U., 1998. Ionospheric response to variable electric fields in small-scale auroral structures. Annales Geophysicae 16, 1343–1354.
Lanchester, B.S., Rees, M.H., Lummerzheim, D., Otto, A., Sedgemore Schulthess, K.J.F., Zhu, H., McCrea, I.W., 2001. Ohmic heating as evidence for strong field-aligned currents in filamentary aurora. Journal of Geophysical Research 106, 1785–1794.
Lanchester, B.S., Rees, M.H., Robertson, S.C., Lummerzheim, D., Galand, M., Mendillo, M., Baumgardner, J., Furniss, I., Aylward, A.D., 2003. Proton and electron precipitation over Svalbard—first results from a new imaging spectrograph (HiTIES). In: Proceedings of the 28th Annual European Meeting on Atmospheric Studies by Optical Methods. Sodankylä Geophysical Observatory Publications 92, 33–36.
Lundin, R., Haerendel, G., Grahn, S., 1998. The Freja mission. Journal of Geophysical Research 103, 4119–4123.
Lysak, R.L., 1990. Electrodynamic coupling of the magnetosphere and ionosphere. Space Science Reviews 52, 33–87.
Maggs, J.E., Davis, T.N., 1968. Measurements of the thicknesses of auroral structures. Planetary and Space Science 16, 205–209.
Marklund, G.T., Ivchenko, N., Karlsson, T., Fazakerley, A., Dunlop, M., Lindqvist, P.-A., Buchert, S., Owen, C., Taylor, M., Vaivads, A., Carter, P., André, M., Balogh, A., 2001. Temporal evolution of the electric field accelerating electrons away from the auroral ionosphere. Nature 414, 724–727.
Massetti, S., 2005. Dayside magnetosphere–ionosphere coupling during IMF clock angle ~90°: longitudinal cusp bifurcation, quasi-periodic cusp-like auroras, and traveling convection vortices. Journal of Geophysical Research (Space Physics) 110, A07304.
McWhirter, I., 2008. Electron Multiplying CCDs—New technology for low light level imaging. In: Proceedings of the 33rd Annual European Meeting on Atmospheric Studies by Optical Methods, Kiruna, Sweden, 28 August–1 September 2006, IRF Scientific Report 292, in print.
McWhirter, I., Furniss, I., Aylward, A.D., Lanchester, B.S., Rees, M.H., Robertson, S.C., Baumgardner, J., Mendillo, M., 2003. A new spectrograph platform for auroral studies in Svalbard. In: Proceedings of the 28th Annual European Meeting of Atmospheric Studies by Optical Methods. Sodankylä Geophysical Observatory Publications 92, 73–76.
Mende, S.B., Eather, R.H., Aamodt, E.K., 1977. Instrument for the monochromatic observation of all sky auroral images. Applied Optics 16 (6), 1691–1700.
Mende, S.B., Frey, H.U., Geller, S.P., Doolittle, J.H., 1999. Multistation observations of auroras: polar cap substorms. Journal of Geophysical Research 104, 2333–2342.
Mende, S.B., Heetderks, H., Frey, H.U., Lampton, M., Geller, S.P., Habraken, S., Renotte, E., Jamar, C., Rochus, P., Spann, J., Fuselier, S.A., Gerard, J.-C., Gladstone, R., Murphree, S., Cogger, L., 2000a. Far-ultraviolet imaging from the IMAGE spacecraft. 1. System design, Space Science Reviews 91, 243–270.

Mende, S.B., Heetderks, H., Frey, H.U., Lampton, M., Geller, S.P., Abiad, R., Siegmund, O.H.W., Tremsin, A.S., Spann, J., Dougani, H., Fuselier, S.A., Magoncelli, A.L., Bumala, M.B., Murphree, S., Trondsen, T., 2000b. Far ultraviolet imaging from the IMAGE spacecraft. 2. Wideband FUV imaging. Space Science Reviews 91, 271–285.

Mende, S.B., Heetderks, H., Frey, H.U., Stock, J.M., Lampton, M., Geller, S.P., Abiad, R., Siegmund, O.H.W., Habraken, S., Renotte, E., Jamar, C., Rochus, P., Gerard, J.-C., Sigler, R., Lauche, H., 2000c. Far ultraviolet imaging from the IMAGE spacecraft. 3. Spectral imaging of Lyman-α and OI 135.6 nm. Space Science Reviews 91, 287–318.

Michell, R.G., Lynch, K.A., Heinselman, C.J., Stenbaek-Nielsen, H.C., 2008. High time resolution AMISR and optical observations of naturally enhanced ion acoustic lines. Annales Geophysicae, submitted for publication.

Moen, J., Burke, W.J., Sandholt, P.E., 1993. A rotating, midday auroral event with northward interplanetary magnetic field. Journal of Geophysical Research 98, 13731–13739.

Murphree, J.S., King, R.A., Payne, T., Smith, K., Reid, D., Adema, J., Gordon, B., Wlochowicz, R., 1994. The Freja ultraviolet imager. Space Science Reviews 70, 421–446.

Obuchi, Y., Sakanoi, T., Ino, T., Asamura, K., Kasaba, Y., Hirahara, M., Okano, S., Ebihara, Y., Seki, K., 2006. Characteristics of black aurora obtained from simultaneous image and particle observations by the REIMEI satellite. American Geophysical Union, Fall Meeting 2006, abstract #SM23B-06.

Oguti, T., 1981. TV observations of auroral arcs. In: Physics of Auroral Arc Formation, Geophysical Monograph Series, vol. 25, American Geophysical Union, pp. 31–41.

Otto, A., Lummerzheim, D., Zhu, H., Lie-Svendsen, Ø., Rees, M.H., Lanchester, B.S., 2003. Excitation of tall auroral rays by ohmic heating in field-aligned current filaments at F region heights. Journal of Geophysical Research (Space Physics) 108, 8017.

Partamies, N., Syrjäsuo, M., Donovan, E., 2007. Using colour in auroral imaging. Canadian Journal of Physics 85, 101–109.

Partamies, N., Syrjäsuo, M., Donovan, E., Knudsen, D., 2008. Dense Array Imaging SYstem prototype observations of missing auroral scale sizes. In: Proceedings of the 33rd Annual European Meeting on Atmospheric Studies by Optical Methods, Kiruna, Sweden, 28 August-1 September 2006. IRF Scientific Report 292, in print.

Pedersen, T.R., Esposito, R.J., Kendall, E.A., Sentman, D., Kosch, M.J., Mishin, E.V., Marshall, R.A., 2008. Observations of artificial and natural optical emissions at the HAARP facility. Annales Geophysicae 26, 1089–1099.

Peticolas, L.M., Hallinan, T.J., Stenbaek-Nielsen, H.C., Bonnell, J.W., Carlson, C.W., 2002. A study of black aurora from aircraft-based optical observations and plasma measurements on FAST. Journal of Geophysical Research 107 (A8).

Pfaff, R., Carlson, C., Watzin, J., Everett, D., Gruner, T., 2001. An overview of the Fast Auroral SnapshoT (FAST) satellite. Space Science Reviews 98 (Issue 1–32).

Røyrvik, O., 1976. Pulsating aurora: local and global morphology. Ph.D. Thesis. University of Alaska, Fairbanks.

Saito, H., Masumoto, Y., Mizuno, T., Miura, A., Hashimoto, M., Ogawa, H., Tachikawa, S., Oshima, T., Choki, A., Fukuda, H., Hirahara, M., Okano, S., 2001. Index: piggy-back satellite for aurora observation and technology demonstration. Acta Astronautica 48, 723–735.

Sakanoi, K., Fukunishi, H., 2004. Temporal and spatial structures of flickering aurora derived from high-speed imaging photometer observations at Syowa Station in the Antarctic. Journal of Geophysical Research 109, A01221.

Sakanoi, T., Okano, Y., Obuchi, Y., Kobayashi, T., Ejiri, M., Asamura, K., Hirahara, M., 2003. Development of the multispectral camera onboard the INDEX satellite. Advances in Space Research 32 (3), 379–384.

Samson, J.C., Cogger, L.L., Pao, Q., 1996. Observations of field line resonances, auroral arcs, and auroral vortex structures. Journal of Geophysical Research 101, 17373–17383.

Sandel, B.R., Broadfoot, A.L., Curtis, C.C., King, R.A., Stone, T.C., Hill, R.H., Chen, J., Siegmund, O.H.W., Raffanti, R., Allred, David, D., Turley, R. Steven, Gallagher, D.L., 2000. The extreme ultraviolet imager investigation for the IMAGE mission. Space Science Reviews 91, 197–242.

Scourfield, M.W.J., Parsons, N.R., 1969. An image intensifier-vidicon system for auroral cinematography. Planetary and Space Science 17, 75–81.

Semeter, J., 2003. Critical comparison of OII(732–733 nm), OI(630 nm), and N_2(1PG) emissions in auroral rays. Geophysical Research Letters, 30 (5), CiteID 1225, doi:10.1029/2002GL015828.

Semeter, J., Blixt, E.M., 2006. Evidence for Alfvén wave dispersion identified in high-resolution auroral imagery. Geophysical Research Letters 33, L13106.

Semeter, J., Vogt, J., Haerendel, G., Lynch, K., Arnoldy, R., 2001a. Persistent quasiperiodic precipitation of suprathermal ambient electrons in decaying auroral arcs. Journal of Geophysical Research 106, 12863–12874.

Semeter, J., Lummerzheim, D., Haerendel, G., 2001b. Simultaneous multispectral imaging of the discrete aurora. Journal of Atmospheric and Terrestrial Physics 63, 1981–1992.

Shiokawa, K., Katoh, Y., Satoh, M., Ogawa, T., Taguchi, M., Yamagishi, H., 2002. New auroral spectrometer using an acousto-optic tunable filter. Advances in Polar Upper Atmosphere Research 16, 146–156.

Stasiewicz, K., Potemra, T., 1998. Multiscale current structures observed by Freja. Journal of Geophysical Research 103, 4315–4326.

Stasiewicz, K., Bellan, P., Chaston, C., Kletzing, C., Lysak, R., Maggs, J., Pokhotelov, O., Seyler, C., Shukla, P., Stenflo, L., Streltsov, A., Wahlund, J.-E., 2000. Small scale Aflvénic structure in the aurora. Space Science Reviews 92, 423–533.

Steen, Å., 1989. An Auroral Large Imaging System in Northern Scandinavia. In: Proceedings of the Ninth Symposium on European Rocket and Balloon Programmes and Related Research, Lahnstein, FRG, ESA SP-291, pp. 299–303.

Stenbaek-Nielsen, H.C., Hallinan, T.J., Osborne, D.L., Kimball, J., Chaston, C., McFadden, J., Delory, G., Temerin, M., Carlson, C.W., 1998. Aircraft observations conjugate to FAST: auroral arc thicknesses. Geophysical Research Letters 25, 2073–2076.

Stenbaek-Nielsen, H.C., Hallinan, T.J., Peticolas, L., 1999. Why do auroras look the way they do? Transactions of the American Geophysical Union (EOS) 80, 193–199.

Streltsov, A.V., 2007. Narrowing of the discrete auroral arc by the ionosphere. Journal of Geophysical Research 112, A10218.

Streltsov, A.V., Lotko, W., 2004. Multiscale electrodynamics of the ionosphere-magnetosphere system. Journal of Geophysical Research 109, A09214.

Størmer, C., 1955. The Polar Aurora. Clarendon Press, Oxford.

Syrjäsuo, M.T., 2001. FMI All-Sky Camera Network. Geophysical Publications, Finnish Meteorological Institute ISBN: 951-697-543-7, ISSN: 0782-6087, 34 pages.

Syrjäsuo, M.T., Jackel, B.J., Donovan, E.F., Trondsen, T.S., Greffen, M., 2005. Low-cost multi-band ground-based imaging of the aurora. In: Fineschi, Silvano, Viereck, Rodney A. (Eds.), Solar Physics and Space Weather Instrumentation. Proceedings of the SPIE, 5901, pp. 113–123.

Taguchi, M., Ejiri, M., Tomimatsu, K., 2004. A new all-sky optics for aurora and airglow imaging. Advances in Polar Upper Atmosphere Research 18, 140–148.

Torr, M.R., Torr, D.G., Zukic, M., Johnson, R.B., Ajello, J., Banks, P., Clark, K., Cole, K., Keffer, C., Parks, G., Tsurutani, B., Spann, J., 1995. A far ultraviolet imager for the international solar-terrestrial physics mission. Space Science Reviews 71, 329–383 (Reprinted in The Global Geospace Mission, ed. By C.T. Russell, Kluwer Academic Publishers, 1995).

Trondsen, T.S., Cogger, L.L., 1997. High-resolution television observations of black aurora. Journal of Geophysical Research 102, 363–378.

Trondsen, T.S., Cogger, L.L., 1998. A survey of small-scale spatially periodic distortions of auroral forms. Journal of Geophysical Research 103, 9405–9416.

Trondsen, T.S., Cogger, L.L., Samson, J.C., 1997. Asymmetric multiple auroral arcs and intertial Alfvén waves. Geophysical Research Letters 24, 2945–2948.

Vogt, J., Frey, H.U., Haerendel, G., Höfner, H., Semeter, J.L., 1999. Shear velocity profiles associated with auroral curls. Journal of Geophysical Research 104, 17277–17288.

Yamamoto, M., Kubota, M., Takeshita, S., Ishii, M., Murayama, Y., Ejiri, M., 2002. Calibration of CRL all-sky imagers using an integrating sphere. Advances in Polar Upper Atmosphere Research 16, 173–180.

Zhu, H., Otto, A., Lummerzheim, D., Rees, M.H., Lanchester, B.S., 2001. Ionosphere–magnetosphere simulation of small-scale structure and dynamics. Journal of Geophysical Research 106, 1795–1806.